



Cite this: *Chem. Commun.*, 2026, **62**, 2820

# Amyloid-based biomaterials: addressing global health, food security and environmental challenges

Hao Su,<sup>ab</sup> Zefeng Gao,<sup>c</sup> Ying Liang,<sup>d</sup> Dongli Ma,<sup>d</sup> Jiwen Zhang<sup>\*ab</sup> and Peng Yang <sup>\*cd</sup>

The growing pressures of population expansion, resource depletion, and climate change are intensifying global challenges in health, food security, and environmental sustainability. Amyloid-based materials offer valuable and sustainable solutions for addressing these issues to achieve a healthier planet due to their controllable structure, exceptional adhesion stability, high mechanical robustness, and excellent environmental compatibility. This review summarizes recent advances in amyloid-based biomaterials with relevance to global health, food, agriculture, and environmental systems. We first discuss the structural characteristics and fabrication strategies of conventional amyloid fibrils and their derived materials. We then introduce a superfast amyloid-like protein aggregation strategy that enables rapid formation of robust protein films and higher-order architectures. Applications of these materials include wound healing and tissue regeneration, stabilization and protection of food systems, enhanced utilization of fertilizers and pesticides, and removal of pollutants from water. Together, these developments highlight the growing potential of amyloid-inspired assemblies as sustainable and scalable platforms for promoting human well-being and environmental resilience.

Received 31st October 2025,  
Accepted 31st December 2025

DOI: 10.1039/d5cc06214d

[rsc.li/chemcomm](http://rsc.li/chemcomm)

## 1. Introduction

The United Nations has projected that the global population will reach 8.6 billion by 2050 and 11.2 billion by 2100.<sup>3</sup> This unprecedented growth, coupled with the accelerating depletion of natural resources and the growing impacts of climate change, is placing immense strain on global systems of health, food security, and environmental sustainability. Escalating issues such as pollution, waste generation, biodiversity loss,

<sup>a</sup> College of Chemistry & Pharmacy, Northwest A&F University, Yangling, 712100, China

<sup>b</sup> State Key Laboratory for Crop Stress Resistance and High-Efficiency Production, College of Plant Protection, Northwest A&F University, Yangling, 712100, China

<sup>c</sup> Key Laboratory of Applied Surface and Colloid Chemistry, Ministry of Education, School of Chemistry and Chemical Engineering, Shaanxi Normal University, Xi'an 710119, China. E-mail: yangpeng@snnu.edu.cn

<sup>d</sup> Xi'an Qingxiu Ecological Technology Co., Ltd., Xi'an 710000, China



**Hao Su**

*Hao Su is a postdoctoral researcher at the College of Chemistry & Pharmacy at Northwest A&F University. Her research interests focus on amyloid-like protein aggregation and sustainable agriculture.*



**Zefeng Gao**

*Zefeng Gao is a Master's student at the College of Chemistry and Chemical Engineering, Shaanxi Normal University. His research focuses on amyloid-like protein aggregation for developing green agricultural inputs and controlling soil pests.*

and uneven human development further exacerbate these interconnected challenges.<sup>17</sup> To address these global challenges, the United Nations established the Sustainable Development Goals (SDGs) in 2015, aiming to achieve a sustainable future for all by 2030.<sup>30</sup> Meeting these challenges requires not only cleaner production and efficient resource management but also the creation of novel material platforms that are inherently sustainable, biodegradable, and environmentally benign. In recent years, both industrial practices and consumer awareness have increasingly favored green and sustainable alternatives over conventional synthetic materials.<sup>36</sup> This shift has driven extensive efforts toward the utilization of renewable resources for the development of biodegradable and environmentally benign materials. Nature provides a rich reservoir of biopolymers, including proteins, starches, cellulose fibers, and lipids, that offer diverse structural and functional characteristics suitable for material innovation.<sup>39,40</sup> Among these, proteins are particularly attractive due to their intrinsic molecular complexity, chemical versatility, and precise self-assembly behavior. As naturally evolved macromolecules, they perform a wide range of biological functions, providing an excellent model for designing biomimetic and functional materials. The structural characteristics and biocompatibility of proteins enable the creation of materials with controlled stability and multifunctionality, making them promising candidates for medical, food, agricultural, and environmental applications.<sup>43,44</sup>

One of the most fascinating manifestations of protein self-assembly is amyloidosis, for example, amyloid fibrils (AF), which are highly ordered  $\beta$ -sheet-rich structures historically associated with human diseases such as Parkinson's, Alzheimer's, Type II diabetes, and others.<sup>46</sup> However, it is now widely recognized that amyloid assemblies are not solely pathological but also serve functional roles in adhesion, melanin synthesis catalysis, peptide hormone storage, and host defense.<sup>47–49</sup> Amyloid

assemblies have emerged as versatile building blocks in nature and engineered systems, inspiring a new generation of sustainable amyloid-based materials due to their exceptional stability, high stiffness, multiple functional groups, and certain bioactivity. Moreover, inspired by natural amyloid fibrils, an amyloid-like strategy was designed by us to assemble natural proteins into amyloid-like protein (ALP) films with excellent environmental compatibility, high mechanical strength, tunable thickness, rapid fabrication efficiency, strong and durable adhesion across various substrates in comparison with other types of amyloids. In recent years, there has been growing interest in the applications of amyloids as templates or building blocks in ordered nanomaterials for biomedical, biomaterial, and nanotechnological applications.<sup>23,50,51</sup> Biomaterials based on amyloid fibrils and amyloid-like protein aggregation have found expanding applications in fields related to human health, food security, and environmental sustainability, demonstrating significant potential for addressing global challenges. In biomedicine, amyloid-based scaffolds have been explored for wound healing, tissue regeneration, and drug delivery. In food and agriculture, amyloid-based materials can serve as natural emulsifiers, stabilizers, or protective coatings for food products while enhancing agrochemical utilization efficiency on crops as adjuvants. In environmental science, amyloid-based materials have been applied as adsorbents and filtration membranes for removing dyes, heavy metals, and organic pollutants from wastewater. All the above broad spectrum of functions and applications of amyloid-based systems originate from their unique structural features, enabling them to operate across a wide range of contexts in both fundamental and applied research. Therefore, it is urgent to compile a comprehensive review to summarize the research studies in these fields. This review aims to provide a comprehensive overview of functional amyloid-based materials, emphasizing their relevance to global health, food security,



**Jiwen Zhang**

*Jiwen Zhang is a professor at the College of Chemistry & Pharmacy at Northwest A&F University. He received his PhD degree from Northwest A&F University in 2013. He conducted visiting research at the Shanghai Institute of Organic Chemistry in 2003, followed by two research stays at the University of Vienna in 2006 and 2014. His research focuses on bioactive natural products, spanning chemical biology and agrochemical applications.*



**Peng Yang**

*Peng Yang is a professor at the School of Chemistry and Chemical Engineering at Shaanxi Normal University. He received his PhD degree from Beijing University of Chemical Technology in 2006. From 2006 to 2012, he conducted postdoctoral research successively at the Department of Colloids and Interfaces of the Max Planck Institute in Germany, Duke University in the United States, and the University of Tokyo in Japan. His research focuses on the development of surface coating and modification systems based on controllable protein aggregation and interfacial adhesion, with the aim of establishing a comprehensive pipeline from fundamental research to industrial applications.*



Scheme 1 Scheme of amyloid-based materials and their applications in human health, food security, and environmental sustainability.

and environmental sustainability (Scheme 1). We first summarize the structure, fabrication strategies, and derived functional materials of conventional amyloid fibrils. Then we outline the superfast amyloid-like protein aggregation strategy, including the construction method, assembly mechanism, and derived functional materials. Subsequently, we explore emerging applications of functional amyloid-based materials, with particular attention to their use in human health, food, agriculture, and environmental systems. Finally, we conclude with an outlook on the challenges and opportunities in translating amyloid-inspired assemblies into practical, scalable solutions for a healthier and more sustainable planet.

## 2. Conventional amyloid aggregates

The rational design and controlled fabrication of amyloid aggregates are fundamental to unlocking their functional versatility and tailoring their performance across biomedical, food/agricultural-related, and environmental applications. Amyloid structures, characterized by their highly ordered cross- $\beta$ -sheet, exhibit exceptional stability, mechanical robustness, and self-assembly capabilities. These properties have inspired their re-engineering into tunable biomaterials with customized physicochemical features. This section discusses the structure, fabrication approaches, and derived functional materials that enable scalable and sustainable production of conventional amyloid fibrils.

### 2.1. Structure and classification of amyloids

Amyloids are a distinct class of protein assemblies defined by their highly ordered fibrillar architecture and exceptional physicochemical stability. Structurally, an amyloid fibril consists of

a rigid core region surrounded by a more flexible flanking domain. The fibril core is typically formed by a subset of residues that adopt a  $\beta$ -sheet conformation and assemble into a continuous cross- $\beta$  spine. The outer flanking segments, which can be intrinsically disordered or partially folded, decorate the fibril surface and confer molecular recognition or functional versatility. The fibrillar core is composed predominantly of extended  $\beta$ -sheets in which the  $\beta$ -strands align perpendicularly to the fibril axis, giving rise to the characteristic cross- $\beta$  diffraction pattern observed by X-ray diffraction.<sup>52,53</sup> This cross- $\beta$  structural motif confers amyloid fibrils with remarkable mechanical rigidity, chemical stability, and proteolytic resistance, setting them apart from other types of protein aggregates. Typically, amyloid fibrils are elongated and unbranched, with diameters in the range of 10–30 nm and lengths in the range of 50–500 nm.<sup>54</sup> The  $\beta$ -sheet stacking distance of approximately 4.8 Å between adjacent strands and 10 Å between neighboring sheets underlies the highly ordered hydrogen-bonding network within the fibril (Fig. 1).<sup>7,55</sup> These features result in exceptional structural stability, as reflected in mechanical moduli reaching  $10^8$ – $10^{10}$  Pa, and in the ability of amyloids to bind specific molecular probes such as Thioflavin T and Congo Red, which are widely used in amyloid identification.<sup>56–59</sup>

From a biological and functional perspective, amyloids can be categorized into pathological, functional, and artificial classes. Pathological amyloids were first recognized in association with degenerative diseases, including Alzheimer's disease (AD), Parkinson's disease (PD), and type II diabetes.<sup>60</sup> Despite significant differences in sequence and native conformation among amyloid  $\beta$  (A $\beta$ ), tau,  $\alpha$ -synuclein, and islet amyloid polypeptide (IAPP), their fibrillar assemblies share the same structural scaffold, demonstrating that a common aggregation pathway underlies these disorders.<sup>61–64</sup> Functional amyloids, in contrast, have been naturally selected to fulfill beneficial biological roles across species.<sup>65</sup> They serve as structural scaffolds



Fig. 1 The structure of an amyloid fibril, which is composed of a rigid fibril core region and a flexible flanking region. The core region adopts a common cross- $\beta$  sheets architecture, while the fibril core formed by different protein subunits displays various topologies with different numbers and spatial arrangements of  $\beta$ -strands. The flanking region displays either a well-folded structure or an intrinsically disordered conformation. Reproduced with permission from Wiley, copyright 2023.<sup>7</sup>

in bacterial biofilms, templates in melanin biosynthesis, storage matrices for peptide hormones, and regulators of long-term memory and intracellular organization.<sup>47,48,66,67</sup> These assemblies are temporally and spatially regulated, reflecting the adaptive evolution of the amyloid fold for specific physiological purposes. Artificial amyloids, on the other hand, are generated under controlled laboratory conditions by inducing denaturation or destabilization of soluble globular proteins. It has been demonstrated that nearly all proteins can form amyloid fibrils once their amyloidogenic segments are exposed, suggesting that the amyloid fold represents a universal and thermodynamically favorable structural motif that may have contributed to early molecular evolution.<sup>68</sup>

Understanding that amyloid formation can occur not only in disease and physiological contexts but also in artificially induced systems provides the foundation for examining how amyloid fibrils can be generated under controlled laboratory conditions. On this basis, the following section summarizes the major experimental strategies used to induce and regulate fibrillation *in vitro*.

## 2.2. Strategies of amyloid fibril formation

Numerous factors could induce the formation of amyloid fibrils, such as pH, ionic strength, temperature, organic reagents, metal ions, and mechanical force. *In vivo*, the key of AD is the assembly of the A $\beta$  into fibrils. It has been reported that AD is linked with inflammation, which can cause acidic micro-environments, and A $\beta$  assembly into fibrils is sensitive to pH.<sup>69</sup> Reduction from physiological pH to a pH closer to the A $\beta$  isoelectric point (pI) of 5.3 will reduce its solubility and so increase self-assembly and the rate of amyloid formation.<sup>70</sup> A $\beta$  accumulates in endo-lysosomal vesicles, where the rate of oligomer formation is accelerated by the low pH.<sup>5,71</sup> *In vitro*, a peptide amphiphile with a cationic pentapeptide segment shows pH-responsive self-assembly. At pH 2, it forms spherical micelles; at pH 3, flat ribbon-like tapes; at pH 4, twisted right-handed helices; and at pH 7, it returns to flat tapes. CD demonstrated a disordered conformation at pH 2 for the spherical micelles and a  $\beta$ -sheet conformation at other pH (Fig. 2A). These reversible pH-induced conformation transitions illustrate the importance of pH for amyloid fibril formation.<sup>72</sup> Song *et al.* discovered that rice protein undergoes distinct aggregation behaviors under varying NaCl concentrations at acidic conditions. At lower salt levels (<100 mM), enhanced electrostatic repulsion promotes the formation of positively charged  $\beta$ -sheet-rich fibrils, while higher concentrations (>100 mM) induce electrostatic shielding, favoring hydrophobic interactions that lead to amorphous aggregates.<sup>73</sup> Nakamura *et al.* demonstrated temperature influenced A $\beta$  production by affecting  $\gamma$ -secretase complex formation. A moderate temperature increase (from 37 °C to 39 °C) enhanced A $\beta$  generation through upregulation of heat shock protein 90 (Hsp90) and presenilin-related components, promoting  $\gamma$ -secretase assembly (Fig. 2B). Similar effects have been confirmed *in vivo*, where higher ambient temperatures elevated Hsp90 and  $\gamma$ -secretase levels in mouse cortex. These findings

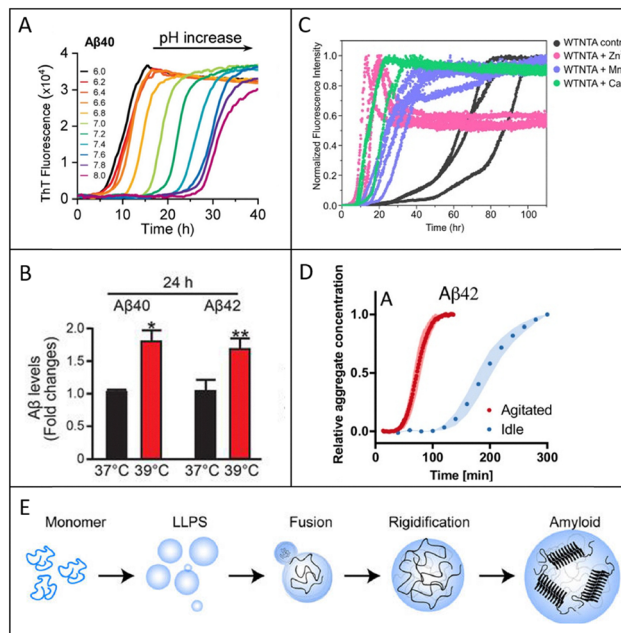


**Fig. 2** (A) pH-dependent fibril formation kinetics of A $\beta$ 40. Reproduced with permission from Wiley, copyright 2022.<sup>5</sup> (B) High temperature increases A $\beta$  production. High temperature increased A $\beta$  production in HEK-APP cells. The levels of A $\beta$ 40 and A $\beta$ 42 in HEK-APP cells were measured with an A $\beta$  ELISA kit. Reproduced with permission from Elsevier, copyright 2020.<sup>22</sup> (C) Metal ions increase the rate of WTNTA  $\alpha$ S amyloid assembly and switch on amyloid formation of  $\Delta\Delta$ NTA  $\alpha$ S. Amyloid assembly of three replicates of WTNTA  $\alpha$ S (gray) alone and in the presence of a 25-fold molar excess of Zn<sup>2+</sup> (pink), Mn<sup>2+</sup> (purple), or Ca<sup>2+</sup> (green). Reproduced with permission from American Chemical Society, copyright 2023.<sup>34</sup> (D) Gentle agitation affects the aggregation kinetics of multiple amyloid proteins. Kinetic traces are shown for four proteins formed with agitation (red) or under idle conditions (blue). Reproduced with permission from National Academy of Sciences, copyright 2024.<sup>38</sup> (E) Schematic representation of the liquid-to-amyloid transition through LLPS. The monomeric protein undergoes self-assembly followed by LLPS, where liquid droplet grows in size through fusion. Protein-rich condensates eventually rigidify with the progressive generation of amyloid aggregates. Reproduced with permission from Royal Society of Chemistry, copyright 2024.<sup>131</sup>

indicated that heat stress modulates A $\beta$  biosynthesis *via* Hsp90-mediated regulation of  $\gamma$ -secretase assembly.<sup>22</sup>

Furthermore, organic reagents like alcohols are widely used to induce and regulate protein fibrillation by modulating hydrophobic and electrostatic interactions. In the case of  $\beta$ -lactoglobulin, solvents such as ethanol and methanol promote the formation of amyloid-like fibrils at specific concentrations, where the balance between solvent-protein interactions and protein-protein associations is optimized. Moderate alcohol levels facilitate partial unfolding and  $\beta$ -sheet rearrangement, favoring ordered fibril formation, while excessive concentrations disrupt this balance, leading to amorphous aggregates. Thus, alcohol-induced fibrillation reflects a delicate interplay between solvent polarity, hydrophobic effects, and protein structural stability.<sup>74</sup> Metal ions play a crucial role in modulating protein conformation and aggregation behavior. For instance,  $\alpha$ -synuclein ( $\alpha$ S), an intrinsically disordered protein, can undergo conformational

transitions upon interaction with divalent metal ions such as  $\text{Ca}^{2+}$ ,  $\text{Mn}^{2+}$ , and  $\text{Zn}^{2+}$ . These ions primarily bind to the C-terminal region of  $\alpha\text{S}$ , inducing structural compaction and promoting the formation of aggregation-prone conformers. Such metal ion-mediated structural rearrangements have been correlated with accelerated amyloid fibrillation, suggesting that metal coordination alters intramolecular interactions and shifts the conformational equilibrium toward aggregation-competent states. This phenomenon highlights the regulatory role of metal ions in protein fibrillization and provides insight into how environmental factors influence amyloid formation (Fig. 2C).<sup>34</sup> Moreover, mechanical forces are increasingly recognized as key physical factors influencing protein self-assembly and fibrillation. Mild agitation or flow can markedly accelerate amyloid formation by promoting both primary and secondary nucleation events. Studies on  $\text{A}\beta_{42}$  and related peptides have shown that shear stress facilitates the detachment of nascent aggregates from catalytic surfaces and enhances molecular transport, thereby increasing the frequency of productive collisions leading to fibril nucleation (Fig. 2D). Although elongation remains largely unaffected, the acceleration of nucleation under gentle agitation highlights the importance of mechanical forces in modulating aggregation kinetics. These findings underscored that hydrodynamic shear not only influences the structural evolution of protein assemblies but also provides valuable insight for controlling amyloid formation in biological and industrial systems.<sup>38</sup>

In addition to the above classical routes that rely on heat, shear, pH shifts, or chemical denaturants, recent experimental work has shown that liquid–liquid phase separation (LLPS) provides an alternative and biologically relevant pathway to amyloid fibril formation. LLPS denotes the reversible demixing of proteins (often together with nucleic acids) from the surrounding cytosol to yield protein-rich, membrane-less condensates or droplets. These condensates create confined microenvironments that differ from the dilute phase in several respects that are directly relevant to fibril formation: local protein concentration is strongly elevated, solvent properties and water activity are altered, molecular diffusion is reduced, and frequent intermolecular contacts are promoted. Such condensates provide a favorable milieu for amyloidogenic proteins to undergo misfolding, oligomerization, and nucleation, ultimately promoting the transition from liquid-like droplets to solid-like amyloid assemblies. Numerous neurodegeneration-related proteins—including tau,  $\alpha$ -synuclein, FUS, TDP-43, and others enriched in intrinsically disordered or low-complexity domains—have been shown to undergo LLPS, where the condensed phase frequently serves as a nucleation crucible for fibril formation (Fig. 2E).<sup>130–134</sup> On the other hand, *in vitro* studies further highlight the regulatory influence of anionic biopolymers on amyloid fibrillization kinetics. For example, polyphosphate modulates  $\text{A}\beta(1–40)$  aggregation in a pH-dependent manner: it inhibits fibril formation at neutral pH but promotes rapid fibrillization through LLPS under acidic conditions, where mature fibrils accumulate within protein-rich droplets. This concentration- and pH-dependent regulation of amyloid formation by polyanions mirrors

intracellular scenarios and provides mechanistic insight into how dysregulated LLPS may contribute to the development and progression of neurodegenerative diseases.<sup>135</sup>

Recent research has shown that a wide variety of proteins are capable of forming amyloid-like fibrils under suitable conditions. Besides the typical pathological proteins, many food- and plant-derived proteins, such as soy protein isolate, zein, gluten, and legume proteins, have been reported to form amyloid-like fibrils when treated under conditions such as low pH, high temperature, or solvent-induced denaturation.<sup>75,76</sup> These findings indicate that the ability to form amyloid fibrils is a general property of many peptides and proteins rather than a feature limited to disease-related proteins. The diversity of fibril-forming food and plant proteins provides a valuable source of sustainable and biodegradable building blocks for developing functional materials in fields such as biomedicine, food technology, agricultural formulations, and environmental sustainability.

### 2.3. Amyloid fibril-based functional materials

Amyloid fibrils have been proven to be an excellent candidate for templating various materials and biotechnological applications, including 1D hybrid materials, films, membranes, hydrogels, and aerogels fabrication. A representative example is the fabrication of Pt–Pd nanoparticle chains using insulin amyloid fibrils as sacrificial templates.<sup>77</sup> When the fibrils are incubated with metal precursors and subsequently reduced, metal nanocrystals nucleate and grow along the fibrillar axis to form continuous 1D chains. These chains retain the linear orientation dictated by the protein scaffold and exhibit enhanced catalytic activity toward CO and methanol oxidation, together with improved tolerance to poisoning when compared with commercial Pt-based catalysts. Similarly, peptide amphiphile assemblies bearing aldehyde groups have been used to organize silver nanoparticles into 1D arrays in aqueous solution (Fig. 3A).<sup>2</sup> The peptide assemblies first form filamentous supramolecular scaffolds, and the aldehyde groups mediate *in situ* reduction of  $\text{Ag}^+$ , yielding silver nanoparticles distributed at regular intervals along the organic filament. The resulting hybrid retains the 1D morphology of the underlying scaffold and shows antibacterial performance while exhibiting lower cytotoxicity toward mammalian cells. This demonstrates that amyloid-inspired 1D templates can support metal nucleation under mild conditions while maintaining compatibility with biological systems.

Amyloid fibrils have also been employed as scaffolds for constructing hybrid membranes with catalytic and separation functions (Fig. 3B).<sup>15</sup>  $\beta$ -lactoglobulin fibrils are first formed in aqueous conditions and subsequently incubated with metal salt precursors, where the fibril surface directs nucleation and controlled growth of metal nanoparticles. Rather than using the hybrid structures solely as dispersed catalysts, the amyloid–nanoparticle complexes are processed into self-supporting membranes through vacuum filtration. When applied in continuous flow reduction reactions, the membranes enable complete conversion of reactants during a single pass of solution,



**Fig. 3** (A) Fabrication of supramolecular nanofibers. Reproduced with permission from American Chemical Society, copyright 2016.<sup>2</sup> (B) Schematic representation of metal nanoparticles-decorated amyloid fibrils and preparation of the catalytically active filter membrane reactor. Reproduced with permission from American Chemical Society, copyright 2015.<sup>15</sup> (C) Fabrication of nanostructured films through multiscale hierarchical self-assembly. (a) Protein molecules are first assembled into amyloid fibrils, which are then stacked into films; (b) atomic force micrograph of the component lysozyme fibrils; (c) scanning electron micrograph of the resulting free-standing protein film. Reproduced with permission from Springer Nature, copyright 2010.<sup>28</sup> (D) Photos and SEM images of the fibril-silica core-shell aerogel (Upper) and silica nanotube aerogel (Lower). Reproduced with permission from National Academy of Sciences, copyright 2019.<sup>37</sup>

demonstrating efficient mass transport, high site utilization, and operational stability. This strategy highlighted how amyloid fibrils can function not only as nanostructural templates but also as structural elements for producing robust membrane materials suitable for continuous chemical processing. Hierarchical assembly of amyloid fibrils further enables the fabrication of ordered 2D films with multiscale structural alignment (Fig. 3C).<sup>28</sup> In a typical procedure, proteins are first assembled into elongated fibrils under conditions that favor intermolecular hydrogen bonding. The fibrils are subsequently cast into thin films, where interactions among fibrils induce in-plane alignment. In the presence of plasticizers, the fibrils further organize into nematic-like layered structures, resulting in materials that exhibit nanoscale order within individual fibrils and micron-scale anisotropy in the film plane. This hierarchical arrangement enhanced mechanical integrity and offers directional control over optical and functional responses.

Moreover, amyloid assemblies can be organized into 3D hydrogels and aerogels with tunable mechanical and biological functions. One illustrative approach is to introduce natural polyphenols into amyloid fibrils that are already present in a nematic state. The polyphenols interact with the fibrils through hydrophobic contacts and hydrogen bonding, driving the formation of interconnected supramolecular networks. The resulting hydrogels retain the orientational order of the precursor fibril suspension and show adjustable stiffness with changes in fibril concentration, pH, and polyphenol content. These hydrogels displayed shear-thinning behavior and thermal stability

across a broad temperature range while also retaining antibacterial activity through membrane disruption. This combination suggested potential use in biomedical environments where both mechanical resilience and antibacterial action are required.<sup>78</sup> In another study, silica is deposited along amyloid fibrils to form core-shell nanofilaments with markedly increased stiffness. Hydrogels formed from these silicified fibrils exhibit elastic moduli several orders of magnitude higher than those of conventional amyloid gels, while preserving network continuity. Through sequential solvent exchange, supercritical drying, and optional removal of the protein core, these hydrogels can be converted into lightweight aerogels with specific surface areas approaching those reported for advanced porous solids, demonstrating a viable route toward structural biomaterials that are both strong and lightweight (Fig. 3D).<sup>37</sup>

### 3. Superfast amyloid-like protein aggregation

Traditional amyloid fibrillation typically requires prolonged incubation under harsh conditions such as high temperature, acidic pH, or the presence of denaturants. However, recent findings suggest that proteins can undergo rapid self-assembly under mild aqueous environments. When the disulfide bonds in proteins are selectively reduced, the resulting conformational flexibility enables spontaneous structural rearrangement. This process can drastically accelerate intermolecular association and  $\beta$ -sheet formation at interfaces, leading to the ultrafast generation of ordered protein architectures. This kind of phase-transition mechanism provides an environmentally friendly route for fabricating functional amyloid-like materials within minutes.

#### 3.1. Fabrication and properties of amyloid-like protein film

In our studies, the fabrication of 2D amyloid-like protein films can be achieved through a spontaneous interfacial assembly process triggered by a reduction-induced phase transition. When lysozyme is dissolved in a neutral buffer containing tris(2-carboxyethyl)phosphine (TCEP), the reduction of intramolecular disulfide bonds leads to conformational unfolding, exposing hydrophobic residues. These partially unfolded oligomers rapidly nucleate and assemble at the air-water and solid-water interfaces, forming a colorless, transparent, continuous, and conformal nanofilm with tunable thickness within minutes under ambient conditions. The assembly proceeds without the need for organic solvents or harsh treatment, reflecting a mild, green, and controllable fabrication route (Fig. 4A).<sup>16</sup>

Direct film formation can be realized by immersing a substrate in the phase transition buffer, where the protein aggregates spontaneously deposit on the contacted region to form a uniform coating. Alternatively, a free-standing film forms at the air-water interface and can be transferred onto solid materials by lifting the substrate through the meniscus or through contact-printing using an agarose hydrogel stamp. This transfer approach allows the coating of both water-tolerant and water-



**Fig. 4** (A) Schematic illustration of the proposed mechanism for the nanofilm formation. (B) (a) Cartoons showing the schematic strategies for the lysozyme nanofilm formation on the surface of immersed materials (solid/liquid interface) and (b) at the aqueous solution surface (vapor/liquid interface). (c) The contact-printing technique to deposit the as-synthesized free-floating nanofilm onto water-sensitive substrates by using agarose hydrogel as a stamp. Reproduced with permission from Wiley, copyright 2016.<sup>16</sup> (C) A cartoon showing different types of main adhesive interactions between the PTL film and versatile material surfaces. Reproduced with permission from Elsevier, copyright 2018.<sup>29</sup> (D) (a) Universality of protein coatings for different materials with various sizes and morphologies; Reproduced with permission from American Chemical Society, copyright 2021.<sup>23</sup> (b–d) Protein coatings coated on the superhydrophobic lotus leaf; reproduced with permission from Wiley, copyright 2022.<sup>20</sup> (e–g) Protein coatings coated on the various wet hydrogel surfaces. Reproduced with permission from American Chemical Society, copyright 2022.<sup>41</sup>

sensitive substrates with defined film geometries (Fig. 4B).<sup>16</sup> The resulting amyloid-like films exhibit strong adhesion to a wide variety of materials, including silicon wafers, metals, and polymers. The densely packed  $\beta$ -sheet structure and the heterogeneous surface chemistry of the film provide numerous active binding sites such as alkyl, aromatic, hydroxyl, carboxyl, thiol, and amine groups, which contribute cooperatively to its universal adhesion behavior. Thus, the interfacial adhesion is primarily attributed to multiple non-covalent interactions between the protein film and the substrate, involving van der Waals forces, metal–sulfur coordination, hydrogen bonding interaction, electrostatic interaction, and hydrophobic interaction. Moreover, the nanostructured roughness of the film enhances the effective contact area and reinforces interfacial bonding strength (Fig. 4C).<sup>29</sup> This phase-transition assembly method can not only uniformly coat micro- and nanoscale objects such as gold, silica, or polystyrene nanoparticles, yeast cells, and CaCO<sub>3</sub> microparticles through simple dispersion in the reactive solution, but can also form on the various macroscopic surfaces, even including superhydrophobic lotus leaf surfaces and highly hydrophilic hydrogels (Fig. 4D).<sup>20,23,41</sup>

The phase-transition strategy for fabricating protein nanofilms is applicable to a wide range of common proteins such as

lysozyme, insulin,  $\alpha$ -lactalbumin, and bovine serum albumin. These proteins share several intrinsic characteristics that enable amyloid-like assembly under reductive conditions. First, their primary structures contain segments with a high propensity for  $\beta$ -sheet formation, which facilitates intermolecular pairing and ordered aggregation. Second, their conformational stability relies heavily on disulfide bonds that maintain the compact  $\alpha$ -helical structure (Fig. 5A).<sup>14</sup> When these bonds are cleaved by reducing agents such as TCEP and cysteine,<sup>79</sup> the native conformation unfolds, exposing hydrophobic and  $\beta$ -prone regions. These residues promote the rapid conversion from  $\alpha$ -helix to  $\beta$ -sheet and drive the formation of  $\beta$ -sheet-rich oligomers that eventually organize into continuous amyloid-like networks at interfaces. This process represents a mild and controllable route for constructing robust 2D protein films.

The resulting amyloid-like nanofilms exhibit outstanding mechanical and adhesion strength (Fig. 5B). When employed as an interfacial binder between a substrate and a metallic layer, the film enhances adhesion by nearly fourfold compared to unmodified surfaces, as demonstrated in peeling and fatigue tests. Even after thousands of stretching and bending cycles, the metal films supported by the protein coating maintain their conductivity and structural continuity, indicating remarkable



Fig. 5 (A) Schematic to show the three key elements in a protein structure leading to superfast amyloid-like assembly. Reproduced with permission from The Royal Society of Chemistry, copyright 2018.<sup>14,23</sup> (B) Schematic diagram of 180° peeling test; diagram showing the relationship between peel strength and peel displacement for the Cu layer on the PTL/SA-modified substrate and the blank substrate. Reproduced with permission from Wiley, copyright 2021.<sup>35</sup> (C) Cell viability of protein coatings. Reproduced with permission from Wiley, copyright 2023.<sup>45</sup>

flexibility and resistance to mechanical fatigue. These properties arise from the densely crosslinked  $\beta$ -sheet framework and the abundant interfacial interactions within the film, which jointly provide excellent load transfer and deformation tolerance.<sup>35</sup> Beyond mechanical robustness, the protein-based phase-transition films display excellent biocompatibility and low ecological risk (Fig. 5C).<sup>8,45</sup> The universality, scalability, and environmental compatibility of this interfacial self-assembly approach make it a versatile platform for fabricating functional protein-based nanofilms.

### 3.2. Mechanism of amyloid-like protein aggregation

The rapid amyloid-like aggregation proceeds by a discrete sequence of molecular events that differs fundamentally from the classical nucleation and growth pathway. The above-mentioned three structural features in typical globular proteins determine whether this superfast pathway is accessible. When these three elements coexist, selective cleavage of disulfide bonds rapidly unlocks the helical domains and exposes hydrophobic and amyloidogenic segments. This abrupt release of monomeric building blocks permits a fast structural conversion from  $\alpha$ -helix to  $\beta$ -sheet and promotes formation of  $\beta$ -rich oligomers and short protofibrils within minutes.

Kinetically, the superfast pathway contrasts with conventional amyloid assembly in two key respects. In typical *in vitro* fibrillation of stable globular proteins, the generation of aggregation competent monomers often requires slow hydrolysis or prolonged denaturation, producing a low effective monomer concentration and a pronounced lag phase before detectable  $\beta$ -sheet growth. By contrast, chemical reduction of disulfide bonds yields unfolded monomers nearly instantaneously, so

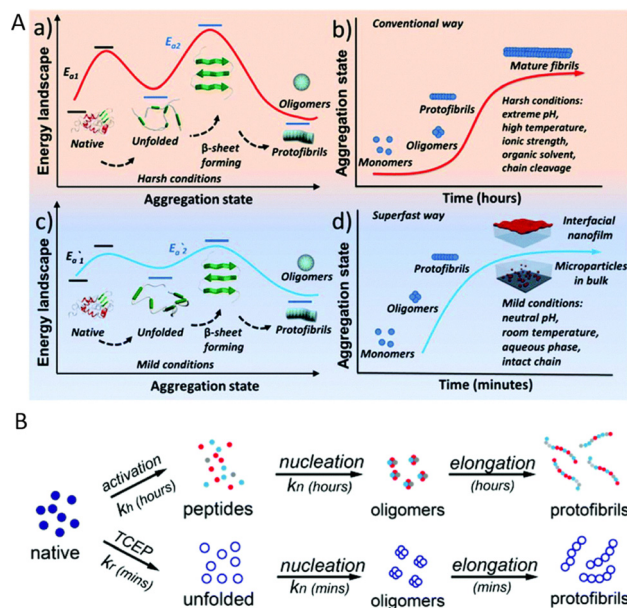


Fig. 6 (A) Schematic process for the conventional amyloid aggregation (a and b) and superfast amyloid-like assembly (c and d). (B) Schematic for conventional and superfast amyloid aggregation. Reproduced with permission from The Royal Society of Chemistry, copyright 2018.<sup>14</sup>

the monomer concentration available for nucleation is close to the initial protein concentration. The result is a greatly accelerated nucleation step and the absence of a long lag phase. Additional modulation arises from colloidal interactions. Raising pH toward the protein isoelectric point reduces electrostatic repulsion among unfolded species, further accelerating hydrophobic association and  $\beta$ -sheet stacking (Fig. 6).<sup>14</sup>

Pathway selection also depends on the interfacial environment. In the rapid aggregation system, oligomeric species formed in solution preferentially enrich at the air–water interface because adsorption lowers interfacial free energy. Interfacial assembly of these oligomers yields continuous two dimensional nanofilms at the interface, while bulk oligomers propagate into protofibrils that may fuse into microparticles in solution. Surface tension measurements, atomic force microscopy, transmission electron microscopy and spectroscopic probes of secondary structure together document this bifurcation of outcome between interfacial film formation and bulk particulate aggregation.<sup>14</sup>

Mechanistic controls and scope were established by comparative experiments. Proteins that combine the three required elements undergo the fast pathway upon reduction, yielding films and microparticles under mild aqueous conditions. Proteins lacking one or more of these elements do not display the rapid  $\beta$ -sheet transition under identical conditions. Spectroscopic evidence shows a rapid increase of hydrophobic exposure followed by a Thioflavin T signal and infrared signatures consistent with  $\alpha$  to  $\beta$  conversion. Molecular dynamics simulations reported in the study further support the role of specific disulfide bonds in enabling the unfolding that precedes  $\beta$ -sheet formation. Together these observations define a

reduction-triggered, interfacial assembly route that is mechanistically distinct from conventional fibrillation.<sup>14</sup>

In summary, the superfast amyloid-like pathway is driven by immediate generation of aggregation competent monomers *via* disulfide bond reduction, rapid  $\alpha$  to  $\beta$  conformational transition, and fast oligomerization. The pathway is accelerated by reduced electrostatic repulsion and guided by interfacial adsorption, producing two dimensional films or bulk micro-particles rather than the slow elongation of long mature fibrils typical of conventional protocols. These mechanistic differences account for both the speed and the distinct material morphologies achievable under mild conditions.

### 3.3. Amyloid-like protein functional materials

Our recent studies have demonstrated that controlled unfolding or phase transition of proteins can induce ultrafast amyloid-like aggregation, enabling the fabrication of high-performance functional materials across 1D and 3D architectures except 2D films.

The ultrafast amyloid-like aggregation of proteins provides a versatile basis for constructing 1D hybrid materials. In one representative strategy, bovine serum albumin is used as a biotemplate to guide the controlled growth of cerium oxide nanorods in aqueous media (Fig. 7A).<sup>1</sup> The protein envelopes the nucleating inorganic phase and modulates its anisotropic crystallization, resulting in uniform nanorods with stable dispersion and abundant surface functional groups. These nanorods

exhibit markedly enhanced photocatalytic hydrogen evolution and CO<sub>2</sub> reduction performance, attributed to promoted interfacial charge transfer and improved adsorption of reactant molecules. This biotemplating route demonstrates the potential of common proteins to direct the morphology and catalytic activity of rare-earth oxide nanomaterials. Another example highlights the ability of amyloid-like assemblies to organize hierarchical biomineralization. A mechanically guided transformation strategy converts phase-transitioned protein films into ordered amyloid-like fibrils with multilayer alignment (Fig. 7B). These fibrils regulate the nucleation and intrafibrillar growth of hydroxyapatite, forming a composite fiber with hardness and elastic modulus comparable to native mineralized tissues. Notably, the mineralized HSAF fibers promote substantial bone regeneration *in vivo*, indicating a combination of structural fidelity and biological functionality. This approach provides a universal route to engineer 1D protein-based fibers with controlled hierarchical structure and high bioactivity.

While 1D fibrillar structures provide mechanical rigidity and directional transport pathways, many functional applications require interconnected networks with continuous phase stability and bulk mechanical integrity. This need has motivated the development of 3D amyloid-like hydrogels and scaffolds based on controlled protein aggregation. Controlled temperature-induced aggregation enables the 3D printing of amyloid-like protein scaffolds (Fig. 7C).<sup>32</sup> The temporary formation of



**Fig. 7** (A) Schematic illustration showing the synthesis of (a) conventional ceria nanorods and (b) PCNRs for photocatalytic systems. Reproduced with permission from Wiley, copyright 2021.<sup>1</sup> (B) A two-step directionally mechanical fabrication of the hierarchically structured amyloid-like fibrils (HSAF) from PTB nanofilm. (a) A schematic of hierarchically structured amyloid-like fibrils; SEM results of (b) surfaces, (c) cross-sections, and (d) corresponding cross-section of the resultant amyloid-like fibrils under different elongation ratios. Reproduced with permission from Wiley, copyright 2025.<sup>6</sup> (C) (a) Schematic diagram of the preparation of the monolithic protein gels using a molding method; (b–d) schematic illustration of the formation mechanisms of three protein gels: PTL gel formed through  $\beta$ -sheet crystallization and chain entanglement (b), PTLC gel formed through calcium ion crosslinking (c), and PTLG gel formed through glutaraldehyde chemical crosslinking (d). Reproduced with permission from Wiley, copyright 2025.<sup>32</sup>

relaxed protein chains allows extrusion into designed geometries, while subsequent  $\beta$ -sheet-rich aggregation establishes stable cross-linking domains that reinforce mechanical integrity. The printed scaffolds exhibit hierarchical ordering and support mineral deposition, demonstrating potential in bone tissue regeneration. This strategy provides a general and tunable pathway for fabricating architected 3D proteinaceous materials with bioactive functionality. These materials are now emerging as functional tools in fields critical to human well-being. Accordingly, we next discuss their applications in global health, food security, and environmental sustainability.

## 4. Applications in global health, food security, and environmental sustainability

The structure-morphology-function relationships outlined in Table 1 clarify how the architectural features of amyloid fibrils and amyloid-like protein assemblies translate into distinct material functions. Building on this framework, the following sections describe representative examples in which these design principles have been integrated into practical solutions for global health, agricultural resilience, and environmental protection. Each example highlights how a particular structural motif—whether the rigidity of 1D nanofibrils, the interfacial adhesion of 2D protein films, or the hierarchical organization of 3D networks—gives rise to the functional advantages observed in real-world applications.

### 4.1. Amyloid-based biomaterials in health

Over the past two decades, biomedical research on amyloids has largely focused on obtaining an improved understanding of the mechanisms causing toxicity in neurodegenerative diseases

and how to inhibit amyloid formation or slow down the process of amyloid-related diseases.<sup>80,81</sup> More recently, it has been found that amyloids have distinct features of self-assembly, structural stability, rich chemical functionality, and mechanical stiffness. Therefore, there has been a growing interest in using non-toxic amyloid-based biomaterials assembled from amyloids for biomedical applications, such as antibacterial and antifouling coating, tissue regeneration, drug delivery, biomineralization, and biomedical glue. Some of the key studies in this area are outlined in this section.

Wang investigated a one-step technique to assemble the model antigen, ovalbumin (OVA), into non-fibrillar OVA globular amyloid aggregates and OVA amyloid-like fibrils as single-component, adjuvant-free vaccines. Notably, the OVA amyloid-like fibrils induced stronger immune responses compared to the native form (Fig. 8A). The efficacy of the vaccine was further validated in a high OVA-expressing tumor model, demonstrating the potential of OVA amyloid-like fibrils as an effective vaccine for cancer immunoprevention.<sup>4</sup> Romano *et al.* showed that bovine alpha-lactalbumin (ALA) amyloid-like fibrils can be used for gastrointestinal delivery of capsaicin (CAP), a pungent compound that exhibits beneficial health effects. The corresponding sustained release of  $7.8 \pm 1.7\%$  to  $55.7 \pm 12.3\%$  CAP occurs under gastric and intestinal conditions. This work presented a new possible avenue for designing protein structures to entrap bioactive moieties.<sup>82</sup> Arghavani *et al.* reported that soy protein isolate amyloid-like aggregates (SPIA) can be used for encapsulating curcumin (Cur) (SPIA@Cur) to enhance its stability and availability, thereby promoting wound healing. *In vivo* experiments in male Wistar rats revealed that both SPIA and SPIA@Cur significantly accelerate wound closure compared with untreated wounds, with SPIA@Cur showing slightly better efficacy.<sup>83</sup> Kabay *et al.* developed a controlled drug release platform by using amyloid-like

**Table 1** Structure-morphology-function relationships for amyloid-based biomaterials

Material morphology	Key structural features	Functional characteristics	Representative application domains
1D amyloid fibrils	<ul style="list-style-type: none"> <li>Highly ordered cross-<math>\beta</math> architecture</li> <li>High aspect ratio and stiffness</li> <li>Dense hydrogen-bonding network</li> </ul>	<ul style="list-style-type: none"> <li>Robust mechanical strength and stability</li> <li>High surface-to-volume ratio for molecular immobilization</li> <li>Efficient charge/energy transfer along fibril axis</li> <li>Strong adhesion to diverse substrates</li> </ul>	<ul style="list-style-type: none"> <li>Antimicrobial materials</li> <li>Catalytic templates</li> <li>Tissue scaffolds</li> <li>Filtration and separation media</li> <li>Pesticide retention and rainfast coatings</li> </ul>
2D amyloid-based films	<ul style="list-style-type: none"> <li>Rapid interfacial assembly driven by disulfide bond reduction and <math>\beta</math>-sheet formation</li> <li>Dense packing of nanoscopic protein oligomers</li> <li>Multipoint, adaptive interfacial interactions (hydrogen bonding, hydrophobic interactions, coordination interactions)</li> </ul>	<ul style="list-style-type: none"> <li>Conformal coverage on complex surfaces</li> <li>High mechanical resilience at the interface</li> <li>Selective permeability and barrier functionality</li> </ul>	<ul style="list-style-type: none"> <li>Food Packaging</li> <li>Anti-biofouling/antimicrobial coatings</li> <li>Personal care and UVshielding films</li> </ul>
3D amyloid-based gels and aerogels	<ul style="list-style-type: none"> <li>Interconnected fibrillar networks</li> <li>Hierarchical pore structure</li> <li><math>\beta</math>-sheet nanocrystals acting as cross-linking nodes</li> </ul>	<ul style="list-style-type: none"> <li>Tunable elasticity and toughness</li> <li>High internal surface area</li> <li>Water and solute transport control</li> <li>Capability for mineralization or nanoparticle incorporation</li> </ul>	<ul style="list-style-type: none"> <li>Biomedical hydrogels for tissue repair</li> <li>Adsorbents for water purification</li> <li>Aerogels for pollutant capture and thermal management</li> <li>Catalytic reactors and sensing platforms</li> </ul>



**Fig. 8** (A) Schematic diagram of OVA assemblies with different structures. Reproduced with permission from Wiley, copyright 2025.<sup>4</sup> (B) (a): Schematic representation of the development of microparticles and their application in the *in vivo* assay; (b): FEG-SEM images of spray-dried AF-HA microparticles. The FEG-SEM experiment was repeated at least three times and a representative image is shown; (c): lesion area of the gastric ulcer in rats. Reproduced with permission from Springer Nature, copyright 2023.<sup>19</sup>

bovine serum albumin (AL-BSA) loaded ampicillin sodium salt (amp).<sup>84</sup> Peydayesh *et al.* designed advanced materials, including films, fibers, and capsules, by the coacervation of  $\beta$ -lactoglobulin AF and hyaluronic acid (HA) for gastric ulcer protection (Fig. 8B).

The properties are by far higher than those of the homologue coacervates obtained by the same constituents but with the protein in its native form, which has great potential in therapeutics and medicine.<sup>19</sup> Palika *et al.* developed a sustainable and biodegradable antiviral filtration membrane composed of milk protein amyloid fibrils and iron oxyhydroxide nanoparticles. The membrane has outstanding efficacy against a broad range of viruses, which include enveloped, non-enveloped, airborne, and waterborne viruses, such as SARS-CoV-2, H1N1, and enterovirus 71.<sup>31</sup> Carvalho *et al.* prepared a self-crosslinkable patch for myocardial implantation through periodate-oxidized nanofibrillated cellulose (OxNFC) blended with lysozyme amyloid nanofibrils (LNFs). The OxNFC:LNFs patch shows superior wet mechanical properties, antioxidant activity, and delivery ability when compared to the patches composed solely of NFC or OxNFC.<sup>85</sup>

Amyloid-based hydrogels can mimic the extracellular matrix and function for tissue engineering, wound healing, and bio-active delivery. Das *et al.* fabricated a pH-responsive self-assembled amyloid hydrogel system to encapsulate growth



**Fig. 9** (A) Representative digital images of skin wounds of two groups at different intervals of time. Reproduced with permission from Wiley, copyright 2025.<sup>10</sup> (B) (a) SEM images and physical appearances of the prepared hybrid hydrogel membranes containing 8 wt% acrylic acid (AA) and 0, 0.5 wt% of WPI amyloid fibrils (WPI-F); (b) Fourier transform infrared (FTIR) spectra of WPI-F and synthesized PAA-WPI-F membranes with different WPI-F contents; (c) compression stress-strain curves. Reproduced with permission from Elsevier, copyright 2025.<sup>24</sup>

factors for driving stem cell differentiation toward neuronal lineage. The results demonstrated that the encapsulated protein molecules can be released in a sustained fashion from the hydrogel over 30 days, and the mesenchymal stem cells cultured in 3D amyloid hydrogels showed more neuron-specific differentiation.<sup>86</sup> Shaw *et al.* investigated a wound dressing composed of peptide-based amyloid hydrogel (Fig. 9A). The corresponding results indicated that it can improve cell migration, proliferation, and collagen remodeling to accelerate wound healing and promote wound closure within 9 and 15 d in both normal and diabetic rats, providing a promising candidate for application in acute and chronic wound healing.<sup>10</sup> Hu *et al.* introduced protein hydrogels developed through the self-assembly of flavonoids and protein amyloid fibrils as a possible approach to mitigate obesity. After oral administration of the hydrogels, high-fat diet (HFD)-induced obesity was significantly prevented in mice, accompanied by downregulation of lipogenesis and pro-inflammatory genes in the liver and adipose tissue and upregulation of lipid metabolism genes. This work provided a general concept to design edible biomaterials for obesity prevention.<sup>87</sup> Chang *et al.* synthesized hybrid hydrogels from whey protein isolate amyloid fibrils (WPI-F) and acrylic acid (AA) (Fig. 9B). The results

highlighted the potential application of WPI-F-reinforced PAA hydrogels in drug delivery systems.<sup>24</sup>

Inspired by traditional amyloid materials, our group developed an amyloid-like protein aggregation strategy to fabricate amyloid-like protein films (ALP) with superior adhesion, rapid formation, and environmental benignity. These films have demonstrated potential as biocompatible wound dressings and antimicrobial/antifouling coatings, combining mechanical strength with safety. Their tunable thickness and substrate compatibility further extend their utility in implant interfaces, tissue protection, biomineralization, hemoperfusion, and regenerative materials. For example, Gu *et al.* reported a phase-transitioned lysozyme (PTL) nanofilm, which exhibited high broad-spectrum antimicrobial efficacy against Gram-positive/negative. Such enhanced antimicrobial capability over native lysozyme is attributed to a synergistic combination of positive charge and hydrophobic amino acid residues enriched

on polymeric aggregates in the lysozyme nanofilm.<sup>88</sup> Hu *et al.* prepared an antifouling phase-transitioned BSA (PTB) coating by one-step aqueous supramolecular assembly of bovine serum albumin (BSA) (Fig. 10A). The nanofilm showed excellent resistance to the nonspecific adsorption of a broad spectrum of contaminants, including proteins, serum, cell lysate, cells, microbes, *etc.* *In vitro/in vivo* experiments showed that the nanofilm can prevent the adhesion of microorganisms and the formation of biofilm.<sup>8</sup> Notably, the antibacterial and antifouling functions can be integrated together by combining ALP with bioactives, thereby enhancing the multiperformance of the material. Tian *et al.* fabricated an antifouling and antibacterial dual-functional coating by using PTB to immobilize  $\epsilon$ -polylysine ( $\epsilon$ -PL) with antibacterial activity and form a coating (PTB@ $\epsilon$ -PL).<sup>89</sup> Wang *et al.* designed a lysozyme (Lyso) and zwitterionic poly(2-methylallyloxyethyl phosphorylcholine) (PMPC) conjugate (Lyso-PMPC) and formed a PTL-PMPC film

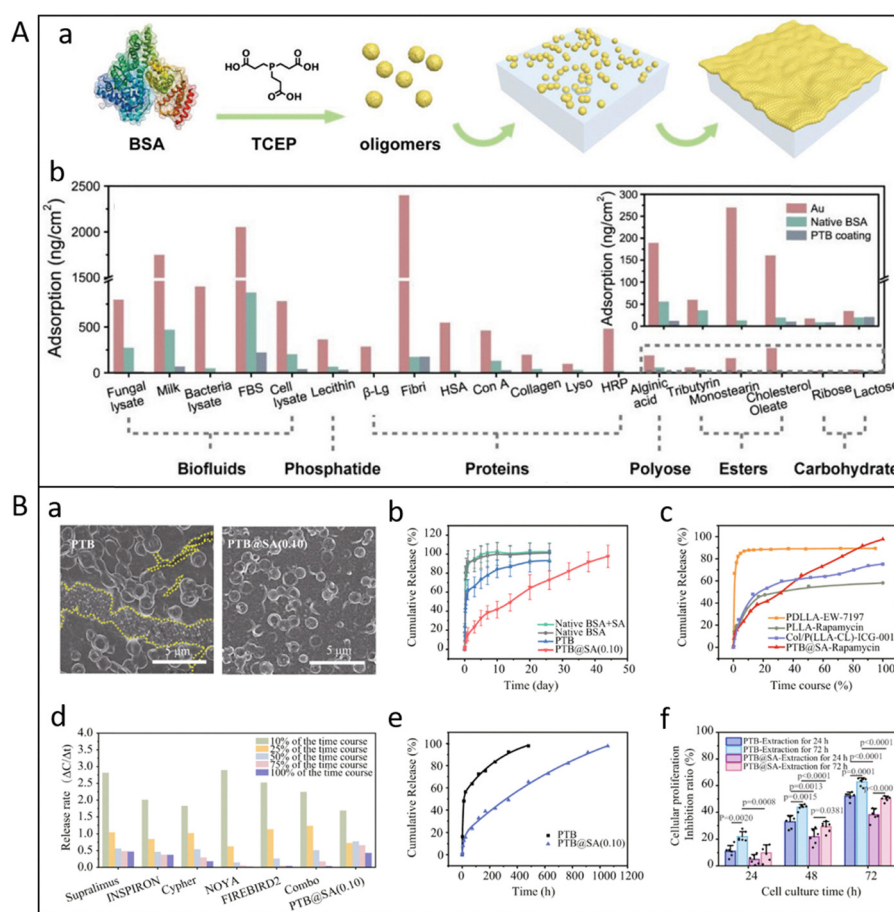


**Fig. 10** (A) (a) Schematic diagram showing the process to form the PTB oligomers and nanofilms at the air-water interface; (b) adsorption amount of biofluids, phosphatide, proteins, polyose, esters, and carbohydrate on bare Au chip, native BSA adsorption layers, or PTB-coated Au chips. Reproduced with permission from Wiley, copyright 2020.<sup>8</sup> (B) (a) SEM image of the rapamycin delivery platform controlled by the PTB or PTB@SA(0.10) nanofilm on SR after releasing into the medium for 14 days; (b) cumulative release of rapamycin from drug reservoirs controlled by different release rate-controlling materials; (c) the time-normalized release profiles of PTB@SA-Rapamycin and other topical delivery systems adapted from the literature for preventing urethral stricture; (d) comparison of the stable release capacity of commercially available rapamycin-eluting stents and PTB@SA-Rapamycin; (e) a biphasic kinetic model was used to fit the release kinetics of rapamycin; (f) the proliferation inhibition ratio of primary rat urethral fibroblasts treated with different extracts as determined by 3-(4,5-dimethylthiazol-2-yl)-2,5-diphenyltetrazolium bromide (MTT) assay. Reproduced with permission from Springer Nature, copyright 2023.<sup>27</sup>

by phase transition of lysozyme *via* the reduction of disulfide bonds in Lyso-PMPC. The PTL-PMPC film had excellent antibacterial efficacy against *Staphylococcus aureus* (*S. aureus*) and *Escherichia coli* (*E. coli*) of more than 99.99%, and antifouling properties against cell, bacterium, fungi, proteins, biofluids, phosphatide, polyose, esters, and carbohydrates.<sup>90</sup>

ALP exhibited strong stability and adhesion with virtually arbitrary substrates, thereby allowing an ultrafast route into practical implications for surface-functionalized commodity and biomedical devices. For instance, Liu *et al.* developed a BSA glue based on amyloid-like protein aggregation. The results showed that a pig's bladder with a 5 mm hole could be patched by BSA glue to withstand 60 cm H<sub>2</sub>O of pressure, and an incision of an SD rat could be closed within 60 s without blood or fluid leakage.<sup>91</sup> Zhao *et al.* developed a stimuli-responsive gauze modified with PTL nanofilm (PTLF@gauze). This PTLF@gauze can be peeled from a mouse wound with less strength, reducing secondary trauma. It can also accelerate wound closure using a murine wound healing model due to the anti-infection properties of PTLF.<sup>92</sup> Du *et al.* utilized our strategy mediated electroless deposition (ELD) technology to deposit silver nanoparticles (Ag NPs) on the cotton fabrics surface in a mild aqueous solution at room temperature, thereby constructing a wearable heater with long-term stability, high conductivity, and exceptional photothermal properties. PTL film and Ag NPs offered textiles excellent antibacterial properties. Therefore, ALP has great promise in areas such as smart wearable clothing and future health management.<sup>93</sup> In addition, ALP exhibited controllable tunability to encapsulate and release functional molecules without significant activity loss. Qin *et al.* developed human lactoferrin (HLF) nanofilm by manipulating the amyloid-like aggregation of HLF and adhered cyclosporin A (CsA)-loaded HLF nanofilms onto the contact lenses (CLs) surface for dry eye syndrome (DES) treatment. These therapeutic CLs displayed a controllable release of CsA when applied to eyes, which improves the CsA bioavailability by at least 82% when compared to the commercial formulation.<sup>41</sup> Tian *et al.* fabricated a PTB/sodium alginate (SA) hybrid nanofilm on the catheter with reliable toughness, which could serve as both a modified coating against bacterial biofilms and a controlled release system to deliver rapamycin in a controlled manner for tens of days (Fig. 10B).<sup>27</sup>

Beyond biomedical coatings and drug release systems, the exceptional surface adhesion and structural tunability of ALP also open avenues for biomimetic mineralization. Biomineralization is a key pathway in nature to grow organic/inorganic hybrid living structures and harnesses the amazing ability to control the formation of biominerals mediated by an organic matrix. For example, Ha *et al.* reported a universal biomimetic mineralization route, PTL coating, that can be applied to virtually any type and morphology of scaffold materials to induce nucleation and growth of hydroxyapatite (HAP) crystals. This method improves the *in vivo* osteoconductivity of Ti-based implants, underpinning the expectation for such biomaterials in future biointerfaces and tissue engineering.<sup>94</sup> Similarly, Gao *et al.* discovered PTL coating could induce biomimetic

mineralization on an implant material, polyetheretherketone (PEEK), significantly enhancing osteogenic capacity when cultured with rat bone marrow mesenchymal stem cells.<sup>95</sup> Wang *et al.* investigated a PTL film mimicking an N-terminal amelogenin with a central domain (N-Ame) combined with a synthetic peptide (C-AMG), which is formed at the enamel interface to induce the synthesis of HAP crystals, thereby facilitating epitaxial growth of HAP crystals, and recovered the highly oriented structure and mechanical properties to levels nearly identical to those of natural enamel. This film provides a promising strategy for treating dental caries.<sup>96</sup> Exposure of dentinal tubules (DTs) usually leads to the transmission of external stimuli within the DTs, causing dental hypersensitivity (DH). Li *et al.* proposed a robust nanofilm through the fast amyloid-like aggregation of lysozyme (lyso) conjugated with poly(ethylene glycol) (PEG) (lyso-PEG). This nanofilm could induce remineralization in the DTs to seal both the orifices and depths of the DTs by forming HAP minerals *in situ* to treat DH. The results showed that the nanofilm-coated DTs are occluded with a depth of over  $60 \pm 5 \mu\text{m}$ , offering an inexpensive, rapid, and efficient therapy for treating DH with long-term effects.<sup>97</sup> Miao *et al.* converts phase-transitioned protein nanofilms into crystalline, hierarchical amyloid-like fibrils with multilayer structures, which effectively control the growth and lateral organization of hydroxyapatite within adaptive gaps. This material exhibited exceptionally high bioactivity in promoting both native bone tissue growth and further intrafibrillar mineralization, achieving 76.9% repair in a mice cranial defect model after 8 weeks and outperforming other regenerative materials (Fig. 11A).<sup>6</sup> Fu *et al.* developed a 3D-printed protein scaffold based on protein gel, which displayed excellent biomineralization capability and had a potential application in bone tissue regeneration using rat skull defect models.<sup>32</sup> ALP-mediated mineralization allows the construction of mechanically reinforced, biocompatible coatings or scaffolds, which have promise for implant interfaces, bone repair, enamel biomineralization, and environmentally benign composite materials.

In addition to serving as a biomimetic template for mineralization, the unique interfacial stability, abundant surface functional groups, high surface area, tunable chemistry, and stable  $\beta$ -sheet network of ALP also endow them with excellent adsorption and separation capacities. Yang *et al.* found that pores with a mean size that can be tailored from 2 to 3 nm are spontaneously formed by adjacent amyloid-like lysozyme oligomers assembled as a nanomembrane at the air/water interface. This PTL membrane with a controllable nanoscale thickness and large area readily supports the excellent hemodialysis performance, especially for the removal of middle-molecular-weight uremic toxins (Fig. 11B).<sup>21</sup> Li *et al.* fabricated an adsorbent by simply mixing lysozyme and SA together, which exhibited high removal efficacy for liver and kidney metabolism wastes, toxic metal ions, and antibiotics, affording great application prospects in the treatment of blood-related diseases.<sup>42</sup>

Overall, the unique combination of structural robustness, tunable functionality, and biocompatibility enables amyloid

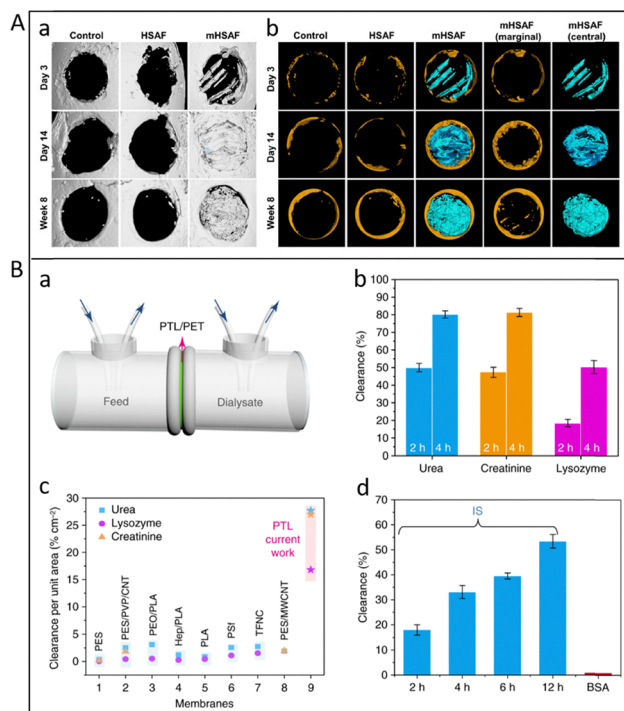


**Fig. 11** (A) (a) Representative micro-CT images and (b) corresponding 3D reconstruction results for the empty control, HSAF, and mHSAF after implantation *in vivo* for 3 days, 14 days, and 8 weeks. Reproduced with permission from Wiley, copyright 2025.<sup>6</sup> (B) (a) The dialysis setup including the simulated solution for dialysis on the feed side and pure water on the dialysis side; (b) size-selective separation of uremic toxins by the PTL/PET membrane: urea, lysozyme and creatinine; (c) comparison of the clearance ratio per unit membrane area of the PTL/PET membrane with typical literature values reported to date; (d) the removal of indoxyl sulfate by the PTL/PET membrane at different times. Reproduced with permission from Springer Nature, copyright 2018.<sup>21</sup>

and amyloid-like protein materials to serve as a versatile platform in biomedical engineering. From surface modification and controlled drug release to biomineralization and blood purification, these materials bridge the gap between natural biological architectures and practical medical applications, offering promising prospects for next-generation biointerfaces and therapeutic devices.

#### 4.2. Amyloid-based biomaterials in agricultural and food-security

The accomplishment of food availability and security for all across sustainable food systems is tied to the Sustainable Development Goals (SDGs). Global food security is also increasingly challenged by crop diseases, excessive agrochemical use, and environmental degradation. Developing safe, efficient, and biodegradable agricultural/food-related materials is essential for sustainable food production. Amyloid-based materials, due to their natural origins, surface activity, mechanical stability, and strong adhesion to biological surfaces, offer promising platforms for controlled emulsion stability, food preservation, agrochemical delivery, and plant protection. Moreover, it has been reported that food amyloids have superior technological,

nutritional, sensorial, and physical properties compared to native monomers, and the digested food amyloids are at least equally as safe as those obtained from the digestion of corresponding native monomers, pointing to food amyloid fibrils as potential ingredients for human nutrition.<sup>98</sup>

Iron fortification of food is a promising strategy to address iron-deficiency anaemia (IDA), a major global public health issue. Shen *et al.* utilized  $\beta$ -lactoglobulin amyloid fibrils as anti-oxidizing nanocarriers and colloidal stabilizers for iron nanoparticles, obtaining a stable protein-iron colloidal dispersion. These iron-amyloid fibril hybrid materials showed high delivery efficacy and *in vivo* iron bioavailability while ensuring primary safety (Fig. 12A).<sup>13</sup> Li *et al.* found that rice glutelin fibrillization would highly improve both the emulsifying and antioxidant abilities of protein dispersion.<sup>99</sup> Chen *et al.* discovered that ultrasonic-mediated pea protein amyloid fibril-epigallocatechin gallate composites exhibited high stability, viscosity, and antioxidant activities, which showed great promise as excellent carriers of bioactive substances, enabling the utilization of pea protein fibril-based hydrogel for stabilizing, encapsulating, and delivering bioactive compounds in food processing.<sup>100</sup> Fu *et al.* reported that ice recrystallization inhibition (IRI) activity is greatly enhanced when AFs serve as Pickering emulsion stabilizers, which provided theoretical and technical support for smart applications of food-grade IRI materials in emulsion-based frozen foods.<sup>101</sup> Oleogelation based on nutritionally valuable ingredients enables liquid oils to target various food and material applications. Therefore, Mykolenko *et al.* proposed a novel approach to design oleogels with high oil content (up to 98%) structured by food protein amyloids at low concentrations. The properties of the amyloid fibrils allow tuning the rheological characteristics, encapsulation efficiency, and interfacial protein concentration in the oleogels for applications in plant-based shortenings, ointments, tissue scaffolds, and controlled-release drug delivery systems.<sup>102</sup> Artificial meat is a promising solution to the negative impacts of meat consumption on natural resources, public health, and animal welfare. Wei *et al.* fabricated a 3D porous scaffold by using soy protein Afs for cultivated meat applications. These food-grade scaffolds can remain stable in phosphate-buffered saline for at least 30 days and enable C2C12 mouse skeletal myoblasts to proliferate and differentiate without adding cell adhesive proteins or other coatings (Fig. 12B).<sup>26</sup>

Beyond their roles in structuring and stabilizing complex food systems, amyloid-based materials also exhibit excellent interfacial stability, antioxidant capacity, and antimicrobial properties, offering new possibilities for extending food shelf life and maintaining nutritional quality during storage. For example, Zeng *et al.* fabricated a multifunctional hydrogel coating by co-assembly of oppositely charged lysozyme AFs and glycyrrhetic acid (GA) nanofibrils through electrostatic interactions and hydrogen bonding. This hydrogel coating displayed excellent gel strength, sprayable capacity, universal surface adhesion, antibacterial and antioxidant efficacy, thereby significantly extending the shelf life to at least 21 days for cherry tomatoes and grapes at ambient temperature.<sup>103</sup>



**Fig. 12** (A) (a) Schematic showing BLG fibrils and the synthesis of iron-BLG fibril nanocomposites; (b) TEM images of pure BLG fibrils and iron-BLG fibril nanocomposites with insets showing their respective suspensions. Reproduced with permission from Springer Nature, copyright 2017.<sup>13</sup> (B) Smart sensor changes over time in a Petri dish in the presence of a shrimp at 4 °C and room temperature (RT). Reproduced with permission from Wiley, copyright 2024.<sup>33</sup>

Similarly, Zheng *et al.* employed a double network hydrogel (DN) coating composed of AF with epigallocatechin gallate (EGCG) and chitosan (CS) and cross-linked using natural genipin (GP) for avocado storage. The DN coating markedly enhanced antimicrobial efficacy against pathogens and extended their shelf life to 12 d while maintaining fruit quality.<sup>104</sup> Yang *et al.* constructed a supramolecular complex (AF-CS-Bet) by combining arachin AFs, CS, and betanin (Bet) to encapsulate cinnamon essential oil (CEO), thereby forming Pickering emulsions for grape preservation. The AF-CS-Bet-CEO emulsion showed higher antioxidant activity and improved antimicrobial activities while exhibiting a better preservation effect.<sup>105</sup> In light of the escalating concerns associated with plastic pollution, considerable research attention has shifted toward the development of protein-based bioplastics as sustainable and eco-compatible alternatives to traditional petroleum-derived polymers. Due to their remarkable mechanical rigidity, intrinsic hydrophobic nature, and exceptional resistance to chemical and thermal degradation, amyloid fibrils have emerged as promising structural components for fabricating renewable and biodegradable plastic materials. For instance, Lai *et al.* utilized zein protein amyloid fibrils (ZPAFs) as sustainable bioplastic films.<sup>106</sup> Dong *et al.* developed electrospun films composed of soy protein

amyloid fibrils (SAFs) and pullulan, significantly improved mechanical strength and antibacterial properties, and afforded opportunities for applications in food systems.<sup>107</sup> More recently, Peydayesh *et al.* demonstrated a film based on whey protein amyloid fibrils functionalized by red radish anthocyanins (RRA) that monitors food spoilage by color change (Fig. 12C). The AM/RRA films can effectively monitor shrimp freshness and exhibit high antibacterial and antioxidant activities, making them promising candidates for contributing to innovations in smart food packaging.<sup>33</sup>

Continuing this line of research, our group further investigated the use of amyloid-like protein assemblies as multi-functional coatings to enhance the preservation and quality maintenance of fresh fruits. Feng *et al.* fabricated an environmentally friendly amyloid-like protein coating through computer-aided molecular simulation in order to address critical challenges in the preservation of perishable fruits, including hydrophobic surface modification, strong adhesion on complex cuticular layers, and the effective combination of multiple preservation components (Fig. 13A). In this system, phase-transitioned lysozyme serves as an adhesive matrix that binds tightly to the fruit epicuticular wax, while sodium alginate and cellulose nanocrystals contribute to the formation of a stable proteinaceous barrier. This coating effectively suppresses microbial growth, reduces moisture loss, and delays spoilage,

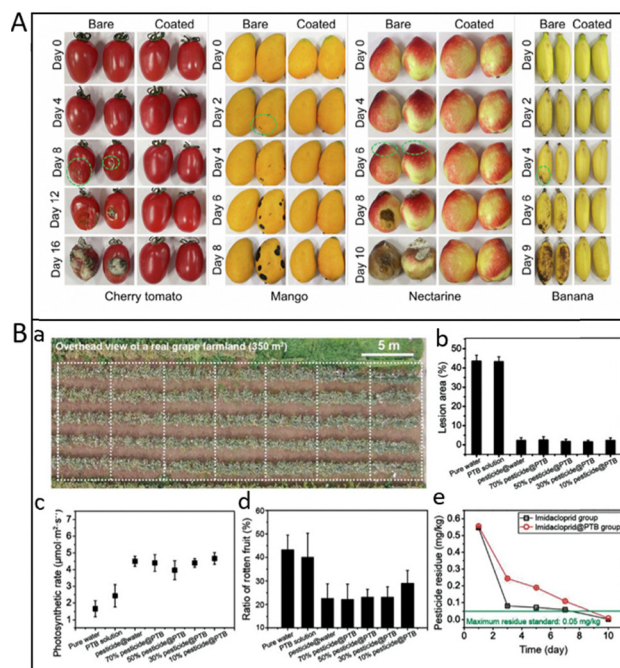


**Fig. 13** (A) Photographs of bare and ALP-coated (spray coating) cherry tomatoes, mangoes, nectarines, and bananas after storage. Reproduced with permission from Springer Nature, copyright 2025.<sup>9</sup> (B) (a–c) The aerial photo (a), lesion area percentage (b), and photosynthetic rate (c) of grape leaves in seven groups; (d) the rotten fruit ratio of grapes in seven groups; (e) time-dependent pesticide residue on corn leaves of imidacloprid in the imidacloprid suspension (Imidacloprid group) and as-prepared PTB solution (Imidacloprid@PTB group). Reproduced with permission from Wiley, copyright 2022.<sup>20</sup>

extending the shelf life of various fruits by 2–4 times while maintaining most of their nutrient content. With its edible nature, low cost, and environmental safety, the coating offers a sustainable alternative to chemical preservatives and significantly reduces carbon emissions compared with traditional refrigeration, highlighting its potential as a practical and sustainable technology for reducing global food waste.<sup>9</sup> Additionally, Liu *et al.* developed a sustainable strategy based on amyloid-like protein aggregation. By immersing fruits in an aqueous solution of lysozyme, L-cysteine, and pectin, a transparent nanocoating forms on the surface, preserving natural appearance while enhancing adhesion and barrier properties. The coating reduces gas and moisture permeability, inhibits microbial growth, and delays browning and firmness loss, extending shelf life from 2 to 4 days at room temperature. Biochemical and biological safety tests confirm minimal oxidative degradation and excellent edibility.<sup>108</sup> Li *et al.* designed a bio-safe superhydrophobic coating composed of PTL with micro-/nano-topography and natural hydrophobic carnauba wax. This coating showed strong interfacial adhesion and enhanced the water repellence of cellulose-based packaging materials to resist the adhesion of milk, yogurt, honey, and various other beverages and edible liquids, which is important to attenuate food spoilage and food waste.<sup>109</sup> Furthermore, Li's group utilized our strategy to prepare the active amyloid membrane ( $\epsilon$ -T-PTL) based on the preparation of amyloid membranes by phase transition lysozyme (PTL) by grafting tannic acid (TA) with lysozyme and mixed  $\epsilon$ -poly-L-lysine ( $\epsilon$ -PL). Finally,  $\epsilon$ -T-PTL displayed excellent preservation properties in delaying snakehead fish oxidation through inhibiting the protein degradation and microbial growth, finally extending the shelf life by 40%.<sup>110</sup>

In addition, amyloid-like protein assemblies have shown strong potential in agricultural applications, particularly in controlled agrochemical delivery and crop protection. Their biodegradability and protein-based origin reduce long-term environmental accumulation, distinguishing them from conventional synthetic polymer adjuvants. Su *et al.* developed a protein-based foliar fertilizer coating in which whey protein concentrate undergoes disulfide bond reduction and subsequent amyloid-like aggregation to form a phase-transitioned WPC (PTW) coating at the solid–water interface. This coating exhibits strong interfacial adhesion and binds fertilizer molecules through electrostatic and hydrogen-bond interactions, enabling uniform deposition and improved retention on hydrophobic leaf surfaces. Field evaluations demonstrated a significant enhancement in fertilizer utilization efficiency, reducing overall fertilizer input by more than 30%.<sup>45</sup>

A related strategy was applied to pesticide formulations, in which disulfide-reduced BSA rapidly forms amyloid-like oligomers that infiltrate leaf surface microstructures and generate stable adhesion. When combined with pesticides, these oligomers markedly increase droplet retention compared to conventional formulations. Field studies further confirmed that pesticide usage can be reduced by 70–90% without compromising yield (Fig. 13B). This protein-mediated interfacial assembly

thus offers an effective approach to improving agrochemical performance while reducing environmental load.<sup>20</sup>

Overall, amyloid-based materials have demonstrated remarkable versatility in addressing challenges in food preservation and agricultural production. Their unique structural and interfacial properties enable the stabilization of complex food systems, extension of fruit shelf life, and improved deposition and bioavailability of fertilizers and pesticides. By combining biocompatibility, environmental safety, and functional performance, these amyloid-based strategies provide effective and sustainable solutions to reduce food spoilage, enhance crop productivity, and minimize chemical inputs in agriculture. Collectively, these advances highlight the potential of amyloid-inspired materials as a transformative platform for promoting food security and sustainable agricultural practices.

### 4.3. Amyloid-based biomaterials in environmental sustainability

The remarkable structural stability, surface reactivity, and tunable self-assembly behavior of amyloid-based materials have extended their utility far beyond biological and food/agricultural systems. In the context of environmental sustainability, these proteinaceous assemblies have been exploited to address urgent ecological challenges such as water purification, precious metal recovery, and the development of biodegradable materials. Due to their high surface area, abundant functional groups, and robustness under harsh physicochemical conditions, amyloid-based materials can serve as efficient adsorbents for pollutants and metal extraction, and renewable substitutes for petroleum-derived plastics. Furthermore, their adaptability in forming stable coatings and composite fabrics enables eco-friendly applications in personal textiles and household materials, supporting a more sustainable industrial and consumer ecosystem.

In recent years, the contamination of aquatic ecosystems has emerged as a pressing global issue. Large quantities of hazardous substances, including heavy metals, organic pollutants, and pathogenic microorganisms originating from industrial, agricultural, medical, and landfill sources, are being released into water bodies at concentrations far exceeding safe limits for human use. Such contamination severely degrades drinking water quality and availability, posing significant threats to environmental safety and public health.<sup>111</sup> To address these issues, Soon *et al.* developed plant amyloid-carbon membranes consisting of sunflower and peanut amyloid fibrils to filter Pt-, Cr-, and Pb-containing water, achieving water of drinkable standards containing < 10 ppb heavy metals.<sup>112</sup> Yang *et al.* extracted plant-derived amyloid fibrils for removing toxic organic dyes from contaminated water with high adsorption capacity.<sup>113</sup> Lu *et al.* prepared three amyloid fibril hybrids—soy protein isolate amyloid fibril-coated ZrO<sub>2</sub> (ZrSAF), lysozyme amyloid fibril-coated ZrO<sub>2</sub> (ZrLAF), and bovine serum albumin amyloid fibril-coated ZrO<sub>2</sub> (ZrBAF)—and evaluated their fluoride removal performance. The results showed that these hybrids demonstrated the fluoride removal capacity in a wide pH range of 3 to 10, and they still had about

89% fluoride ion removal efficiency after five adsorption cycles even in real wastewater experiments.<sup>114</sup> Zeng *et al.* synthesized a mixed-linker L-histidine@zeolitic imidazole framework-8 (His@ZIF-8) layer on the amyloid nanofibril (ANF)-modified hydrolyzed polyacrylonitrile (HPAN) membrane, thereby facilitating the tuning of surface and molecular sieving properties of ZIF-8 on the membranes and improving the overall separation and antifouling performance of the His@ZIF-8/ANFs membrane. The resultant His@ZIF-8/ANF membrane exhibits higher water flux, superior heavy metal ion ( $\text{Cu}^{2+}$ ,  $\text{Ni}^{2+}$ ,  $\text{Pb}^{2+}$ , and  $\text{Cd}^{2+}$ ) rejection, and higher antibacterial efficiency, making it a suitable material for wastewater treatment applications.<sup>115</sup>

In addition to membrane materials, amyloid-based materials have been further advanced into aerogel architectures, such as aerogel and sponge, enabling enhanced mass transfer, adsorption efficiency, and multifunctionality in complex water purification scenarios. For example, Jia *et al.* developed amyloid fibrils/ZIF-8 hybrid aerogels through a metal-organic framework (MOF) crystallization functionalized amyloid fibril to remove nine different heavy metal ions from water. The resulting aerogels exhibited high specific area, broad functionality, and mechanical strength, and showed high removal efficacy even after five consecutive cycles.<sup>116</sup> Tu *et al.* fabricated 3D carboxymethyl cellulose (CMC) or chitosan (CS)-modified whey protein amyloid fibril (WPIAF) aerogels for oil/water separation and emulsion separation. The WPIAF aerogel demonstrated enhanced mechanical strength, elevated surface hydrophobicity, and superior performance in oil and emulsion separation. Its high adsorption efficiency and recyclability highlight the potential of amyloid-based aerogels as effective materials for oil/water separation and emulsion separation.<sup>117</sup> Peydayesh *et al.* fabricated aerogel adsorbers from the 2 wt%  $\beta$ -lactoglobulin aqueous amyloid fibril dispersion by freeze-drying the cross-linked gel. The resulting aerogel showed excellent removal efficiencies of model organic pollutants, such as Bentazone, Bisphenol A, and Ibuprofen. This aerogel showed great promise for potential applications in removing organic pollutants from wastewater (Fig. 14A–F).<sup>11</sup> Moreover, they prepared carbon aerogels combining whey protein isolate amyloid fibrils and different carbohydrates, which displayed excellent removal efficiencies for adsorbing Au(III), Pt(II), Fe(III), and Ag(I). Both of the above two aerogels showed high reusability even after 3 consecutive cycles.<sup>118</sup> Furthermore, they have explored whey amyloid fibril aerogels as adsorbents for gold recovery from e-waste. The aerogels exhibited remarkable gold adsorption capacity and selectivity, while they can convert gold ions into single crystalline flakes due to Au growth along the (111) plane.<sup>119</sup>

Amyloid-based assemblies have shown significant promise in addressing environmental pollution through adsorption and separation. Amyloid fibrils carrying alkylamine groups can reversibly bind carbon dioxide through carbamate formation, achieving efficient and regenerable  $\text{CO}_2$  capture even in humid conditions (Fig. 14G–L).<sup>25</sup> Whey-derived hybrid amyloid aerogels have also been developed for solar-driven desalination and wastewater purification. These materials combine rapid water

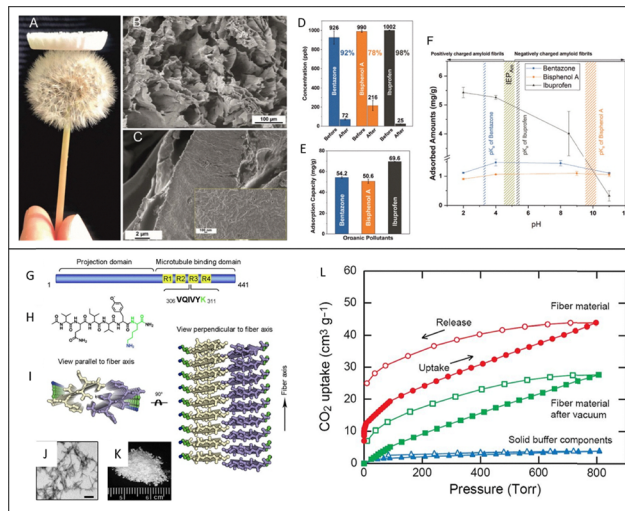


Fig. 14 (A) Photograph of an amyloid fibril aerogel produced by freeze-drying on top of dandelion flower seeds. (B and C) Cross-section SEM images of the aerogel as an overview and in detail of the wall of a pore. (D) Concentrations of organic pollutants before and after adsorption by an amyloid fibril aerogel. (E) The adsorption capacity of an amyloid fibril aerogel for organic pollutants. (F) Effect of pH on organic pollutant adsorption by an amyloid fibril aerogel. Reproduced with permission from Wiley, copyright 2020.<sup>11</sup> (G) Schematic of tau protein, with its repeat regions (R1–R4) in the microtubule binding domain. (H) Chemical structure of capped VQIVYK showing its N-terminal acetylation and C-terminal amidation. (I) Crystal structure of uncapped VQIVYK (PDB ID 2ON9). (J) TEM image of amyloid fibers formed by capped VQIVYK. Scale bar, 300 nm. (K) Dry powder of the VQIVYK fiber. (L) Carbon dioxide adsorption isotherms for the VQIVYK fiber material. Reproduced with permission from National Academy of Sciences, copyright 2013.<sup>25</sup>

transport and strong photothermal conversion, effectively removing heavy metals, organic pollutants, and pathogens while producing clean water under mild solar illumination.<sup>120</sup> Amyloid fibrils derived from food waste have been successfully utilized as structural components for biodegradable films. By integrating soy whey and okara proteins with methylcellulose and glycerol, transparent and flexible bioplastics were produced on an industrial scale. These films exhibit mechanical strength and moisture resistance comparable to conventional plastics while being fully biodegradable. This approach not only mitigates plastic pollution but also adds value to agricultural residues, offering a feasible pathway for circular bioeconomy development.<sup>121</sup> Beyond material valorization, amyloid-based coatings and nanostructures are also contributing to sustainable textile innovation. A composite system combining lysozyme-derived amyloid coatings, molybdenum disulfide nanosheets, and *in situ* reduced silver nanoparticles achieved nearly complete bacterial inactivation, maintained even after extensive washing. These materials integrate photothermal, oxidative, and ionic antibacterial mechanisms, providing long-lasting protection with good biocompatibility. Such examples highlight the potential of amyloid-inspired materials to promote safer and more sustainable applications in personal care and environmental hygiene.<sup>122</sup>

In response to the growing global emphasis on sustainability and environmental protection, and building upon these advances, our group has broadened the application of ALP to a wide range of green technologies. These studies demonstrate that the phase-transitioned protein structures, with their tunable surface chemistry, robust adhesion, and excellent biocompatibility, can serve as universal molecular tools for constructing green materials across multiple environmental interfaces.

In the field of pollution control and water purification, ALP-based adsorbents and composites have been developed to remove a variety of hazardous pollutants. Yang *et al.* prepared a PTB-sodium CMC complex through amyloid-mediated coacervation, which exhibited rapid and efficient removal of multiple toxic metal ions and radioactive elements from water within minutes, meeting WHO standards.<sup>123</sup> Similarly, a PTL- $\beta$ -cyclodextrin (PTL- $\beta$ -CD) composite enabled selective and high-capacity uranium extraction from aqueous media, outperforming conventional adsorbents in both efficiency and cost-effectiveness.<sup>124</sup> To address polymer leakage pollution, a PTL coating was formed on the wire mesh surface with the decoration of 2,2,6,6-tetrame thylpiperidin-1-oxyl (TEMPO)-oxidized cellulose nanocrystals (CNC) to fabricate a superpolymphobic coating. This superpolymphobic coating was further utilized to efficiently separate viscous liquid polymers from water with 99.49% separation efficiency and exceptional mechanical stability, providing a scalable solution for industrial wastewater treatment.<sup>125</sup>

Beyond pollutant removal, ALP-based systems have also demonstrated remarkable potential in precious metal recovery and resource recycling. Through PTB-mediated surface engineering, industrial solid wastes such as fly ash, clay, resin, and  $\text{Al}_2\text{O}_3$  were converted into highly efficient adsorbents for noble metal capture, achieving adsorption capacities tens to thousands of times higher than traditional adsorbents and dramatically increasing the economic value of waste materials.<sup>126</sup> Protein-based phase-transition membranes, such as PTL and PTB, have also been successfully applied to the selective recovery of gold and other precious metals from ores, electronic waste, and industrial leachates (Fig. 15A).<sup>12,127</sup> These biosorbents exhibited high selectivity and recyclability, thus offering an energy-efficient and sustainable strategy for circular resource utilization.

In parallel, our group has explored ALP-based materials for mitigating environmental pollution from daily living equipment. A PTL/SA coating effectively prevented plasticizer migration from medical and food plastics, achieving a reduction of up to 99.9% while maintaining interfacial stability under mechanical stress.<sup>128</sup> For domestic sustainability, Feng *et al.* developed a PTL/CNC hybrid coating for detergent-free oil removal from tableware, reducing water and energy consumption by more than 50% compared with conventional cleaning (Fig. 15B).<sup>18</sup> Similarly, a PTL/zwitterionic poly(sulfobetaine methacrylate) (pSBMA) conjugated coating imparted superoleophobicity to textiles, creating self-cleaning and detergent-free fabrics that substantially lower the environmental footprint of

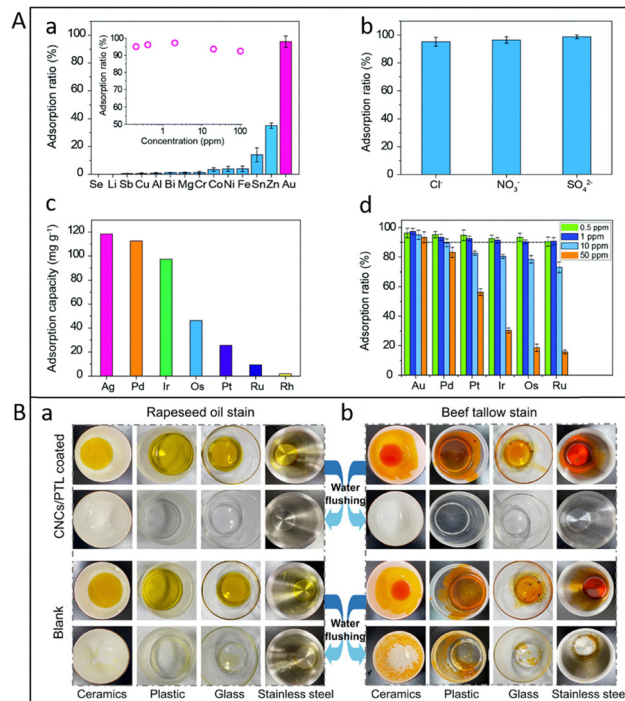


Fig. 15 (A) (a) The effect of competing metal ions (100 ppm each) on gold ion adsorption; the inset shows the adsorption of gold ions with different concentrations in a mixed metal ion solution; (b) the effect of  $\text{Cl}^-$ ,  $\text{NO}_3^-$  and  $\text{SO}_4^{2-}$  (0.01 M) on gold adsorption; (c) adsorption capacity of the membrane for precious metals in a single system; (d) effect of initial precious metal ion concentration on adsorption in a mixed system. Reproduced with permission from The Royal Society of Chemistry, copyright 2020.<sup>12</sup> (B) Photographs of the CNC/PTL-coated and blank bowls contaminated with (a) rapeseed oil and (b) beef tallow before and after water rinsing. Reproduced with permission from Wiley, copyright 2024.<sup>18</sup>

laundry operations.<sup>129</sup> Chang *et al.* created leakage-resistant sunscreens that prevent synthetic UV filters from entering aquatic ecosystems while maintaining long-term skin protection under seawater exposure. These systems integrate structural robustness, ecological safety, and user compatibility, presenting an innovative paradigm for sustainable material design.

Collectively, these studies highlight the versatility of amyloid-like protein materials as a universal molecular engineering platform. From pollution abatement and resource recovery to eco-friendly coatings and consumer product sustainability, the amyloid aggregation principle provides a unifying framework to construct robust, green, and high-performance materials that align with the goals of environmental protection and circular economy.

## 5. Conclusions and outlook

This review has provided a comprehensive overview of amyloid-based biomaterials, focusing on their design principles, assembly mechanisms, and diverse applications in human health, agriculture, food safety, and environmental sustainability. Through the examples discussed, including both established

and emerging studies as well as the recent advances achieved by our group, it becomes clear that protein self-assembly offers a versatile and sustainable strategy for creating functional materials with tunable structures, strong interfacial adhesion, and inherent biocompatibility. These attributes place amyloid-based materials at the frontier of green innovation, resonating with the vision of Environmental Science for a Healthier Planet.

Despite their promising potential, several critical challenges remain before these materials can reach widespread application. The first lies in scalable and sustainable production. The cost and consistency of protein resources, as well as the reproducibility of large-scale assembly, require further optimization to meet industrial standards. The second concerns biosafety and environmental impact, which demand systematic evaluation of degradation behavior, ecotoxicity, and long-term stability under realistic conditions such as soil, aquatic, and atmospheric exposure. The third challenge involves durability and multifunctionality. In real-world scenarios, materials must retain their properties under ultraviolet radiation, microbial activity, and mechanical wear while achieving multiple performance goals simultaneously or safety and reusability in consumer products.

Addressing these challenges calls for an integrated research and development framework. Future work should prioritize the use of renewable and low-cost protein resources, particularly those derived from plant- and food-processing byproducts, thereby linking material innovation with circular bioeconomy goals. Advances in process intensification and scalable fabrication can enhance reproducibility and facilitate industrial implementation. Establishing standardized assessment protocols covering physicochemical performance, degradation kinetics, and toxicological safety will be essential for cross-comparison and regulatory approval. Furthermore, the incorporation of computational modeling, machine learning, and high-throughput screening may accelerate the discovery of sequence–structure–function relationships, enabling rational design at the molecular level. Equally important is the inclusion of life cycle assessment from the outset, ensuring that the environmental footprint of new materials remains lower than that of conventional counterparts throughout production, use, and disposal.

The translation of amyloid-based technologies into practice will depend on close interdisciplinary and cross-sector collaboration. Academic researchers, industrial partners, agricultural producers, and regulatory bodies must jointly develop pilot-scale platforms to validate performance and environmental compatibility under real conditions. Policymakers and funding agencies can play a vital role in supporting scale-up demonstrations, methodological standardization, and the establishment of sustainable supply chains. Public engagement and education should also be strengthened to ensure social acceptance and to align innovations with societal needs.

From a broader perspective, amyloid-based materials can be regarded as a promising direction in developing environmentally compatible biomaterials. By aligning high performance with environmental harmony, they have the potential to contribute to global efforts addressing human health, food

security, and environmental sustainability. With rigorous science, responsible translation, and supportive policy frameworks, amyloid-based biomaterials could become an important technology in the common pursuit of a cleaner, safer, and more sustainable planet.

## Author contributions

All authors contributed to the conceptualization, writing and editing of this feature article.

## Conflicts of interest

There are no conflicts to declare.

## Data availability

No primary research results, software or code have been included and no new data were generated or analysed as part of this review. All data supporting this article are available from the cited literature.

## Acknowledgements

We are grateful for funding from the National Science Fund for Distinguished Young Scholars (No. 52225301), the National Key R&D Program of China (No. 2020YFA0710400 and 2020YFA0710402), the Key Project of Shaanxi Province-Research on Key and Core Technologies in Agriculture and Rural Areas (No. 2024NC-GJHX14), the Qinchuangyuan “Scientist + Engineer” Team Development Project of Shaanxi Province (No. 2023KXJ-124), the Key Agricultural Industry Chain Technology Research Project of Xi’an City (No. 23NYGG0004), the National Natural Science Foundation of China (No. 52403143), the Postdoctoral Research Funding Project of Shaanxi Province (No. 2024BSHSDZZ071), and the Postdoctoral Fellowship Program of CPSF (No. GZC20241392).

## References

- 1 B. Saif, Q. Gu and P. Yang, *Small*, 2021, **17**, 2103422.
- 2 E. Pazos, E. Sleep, C. M. Rubert Perez, S. S. Lee, F. Tantakitti and S. I. Stupp, *J. Am. Chem. Soc.*, 2016, **138**, 5507–5510.
- 3 J. Bongaarts, *Nature*, 2016, **530**, 409–412.
- 4 X. Wang, H. Xia, T. Li, Q. Zuo, Z. Wang, K. Yan, Z. Xu, W. Xue, G. Sun and Z. Liu, *Adv. Healthcare Mater.*, 2025, **14**, 2401625.
- 5 Y. Tian and J. H. Viles, *Angew. Chem.*, 2022, **134**, e202210675.
- 6 S. Miao, J. Guo, Y. Zhang, P. Liu, X. Chen, Q. Han, Y. Wang, K. Xuan, P. Yang and F. Tao, *Adv. Mater.*, 2025, 2416824.
- 7 Q. Xu, Y. Ma, Y. Sun, D. Li, X. Zhang and C. Liu, *Aggregate*, 2023, **4**, e333.
- 8 X. Hu, J. Tian, C. Li, H. Su, R. Qin, Y. Wang, X. Cao and P. Yang, *Adv. Mater.*, 2020, **32**, 2000128.
- 9 N. Feng, J. Zhang, J. Tian, Y. Zhang, M. Li, X. Guo, Q. Han, Y. Wang, A. Gao and Y. Wang, *Nat. Commun.*, 2025, **16**, 5060.
- 10 R. Shaw, K. Patel, N. M. Chimthanawala, S. Sathaye and S. K. Maji, *Adv. Healthcare Mater.*, 2025, **14**, 2403560.
- 11 M. Peydayesh, M. K. Suter, S. Bolisetty, S. Boulos, S. Handschin, L. Nyström and R. Mezzenga, *Adv. Mater.*, 2020, **32**, 1907932.

- 12 F. Yang, Z. Yan, J. Zhao, S. Miao, D. Wang and P. Yang, *J. Mater. Chem. A*, 2020, **8**, 3438–3449.
- 13 Y. Shen, L. Posavec, S. Bolisetty, F. M. Hilty, G. Nyström, J. Kohlbrecher, M. Hilbe, A. Rossi, J. Baumgartner and M. B. Zimmermann, *Nat. Nanotechnol.*, 2017, **12**, 642–647.
- 14 C. Li, L. Xu, Y. Y. Zuo and P. Yang, *Biomater. Sci.*, 2018, **6**, 836–841.
- 15 S. Bolisetty, M. Arcari, J. Adamcik and R. Mezzenga, *Langmuir*, 2015, **31**, 13867–13873.
- 16 D. Wang, Y. Ha, J. Gu, Q. Li, L. Zhang and P. Yang, *Adv. Mater.*, 2016, **28**, 7414–7423.
- 17 P. Khatri, P. Kumar, K. S. Shakya, M. C. Kirlas and K. K. Tiwari, *Environ. Dev. Sustainability*, 2024, **26**, 24107–24150.
- 18 N. Feng, X. Chen, Q. Han, Y. Liu, L. Yan, A. Gao and P. Yang, *Aggregate*, 2024, **5**, e465.
- 19 M. Peydayesh, S. Kistler, J. Zhou, V. Lutz-Bueno, F. D. Victorelli, A. B. Meneguín, L. Spósito, T. M. Bauab, M. Chorilli and R. Mezzenga, *Nat. Commun.*, 2023, **14**, 1848.
- 20 H. Su, Y. Liu, Y. Gao, C. Fu, C. Li, R. Qin, L. Liang and P. Yang, *Adv. Sci.*, 2022, **9**, 2105106.
- 21 F. Yang, F. Tao, C. Li, L. Gao and P. Yang, *Nat. Commun.*, 2018, **9**, 5443.
- 22 A. A. Noorani, H. Yamashita, Y. Gao, S. Islam, Y. Sun, T. Nakamura, H. Enomoto, K. Zou and M. Michikawa, *J. Biol. Chem.*, 2020, **295**, 18010–18022.
- 23 Y. Liu, F. Tao, S. Miao and P. Yang, *Acc. Chem. Res.*, 2021, **54**, 3016–3027.
- 24 C. Y. Chang, T. L. Hsu, Y. R. Lai, J. W. Wu, S. S. S. Wang, S. C. How and T. H. Lin, *J. Drug Delivery Sci. Technol.*, 2025, 107299.
- 25 D. Li, H. Furukawa, H. Deng, C. Liu, O. M. Yaghi and D. S. Eisenberg, *Proc. Natl. Acad. Sci. U. S. A.*, 2014, **111**, 191–196.
- 26 Z. Wei, S. Dai, J. Huang, X. Hu, C. Ge, X. Zhang, K. Yang, P. Shao, P. Sun and N. Xiang, *ACS Appl. Mater. Interfaces*, 2023, **15**, 15108–15119.
- 27 J. Tian, D. Fu, Y. Liu, Y. Guan, S. Miao, Y. Xue, K. Chen, S. Huang, Y. Zhang and L. Xue, *Nat. Commun.*, 2023, **14**, 2816.
- 28 T. P. Knowles, T. W. Oppenheim, A. K. Buell, D. Y. Chirgadze and M. E. Welland, *Nat. Nanotechnol.*, 2010, **5**, 204–207.
- 29 J. Gu, S. Miao, Z. Yan and P. Yang, *Colloid Interface Sci. Commun.*, 2018, **22**, 42–48.
- 30 M. E. Mondejar, R. Avtar, H. L. B. Diaz, R. K. Dubey, J. Esteban, A. Gómez-Morales, B. Hallam, N. T. Mbugu, C. C. Okolo and K. A. Prasad, *Sci. Total Environ.*, 2021, **794**, 148539.
- 31 A. Palika, A. Armanious, A. Rahimi, C. Medaglia, M. Gasbarri, S. Handschin, A. Rossi, M. O. Pohl, I. Busnadiego and C. Gübeli, *Nat. Nanotechnol.*, 2021, **16**, 918–925.
- 32 C. Fu, Y. Pang, J. Zhang, X. Zhou, Y. Liu, M. Li, J. Song, Y. Gao, Z. Wang and B. Hu, *Adv. Funct. Mater.*, 2025, **35**, 2420569.
- 33 M. Peydayesh, A. Kovacevic, L. Hoffmann, F. Donat, C. Wobill, L. Baraldi, J. Zhou, C. R. Müller and R. Mezzenga, *Adv. Mater.*, 2025, **37**, 2414658.
- 34 E. J. Byrd, M. Wilkinson, S. E. Radford and F. Sobott, *J. Am. Soc. Mass Spectrom.*, 2023, **34**, 493–504.
- 35 M. Chen, F. Yang, X. Chen, R. Qin, H. Pi, G. Zhou and P. Yang, *Adv. Mater.*, 2021, **33**, e2104187.
- 36 A. T. Nguyen, L. Parker, L. Brennan and S. Lockrey, *J. Cleaner Prod.*, 2020, **252**, 119792.
- 37 Y. Cao, S. Bolisetty, G. Wolfisberg, J. Adamcik and R. Mezzenga, *Proc. Natl. Acad. Sci. U. S. A.*, 2019, **116**, 4012–4017.
- 38 E. Axell, J. Hu, M. Lindberg, A. J. Dear, L. Ortigosa-Pascual, E. A. Andrzejewska, G. Šneiderienė, D. Thacker, T. P. Knowles and E. Sparr, *Proc. Natl. Acad. Sci. U. S. A.*, 2024, **121**, e2322572121.
- 39 Y. Zhang, *Processing and Development of Polysaccharide-Based Biopolymers for Packaging Applications*, Elsevier, 2020.
- 40 L. Averous and E. Pollet, *Environmental Silicate Nano-Biocomposites*, Springer, 2012.
- 41 R. Qin, Y. Guo, H. Ren, Y. Liu, H. Su, X. Chu, Y. Jin, F. Lu, B. Wang and P. Yang, *ACS Central Sci.*, 2022, **8**, 705–717.
- 42 M. Li, M. Chen, F. Yang, R. Qin, Q. Yang, H. Ren, H. Liu and P. Yang, *Adv. Healthcare Mater.*, 2023, **12**, 2300999.
- 43 J. F. Diaz-Villanueva, R. Díaz-Molina and V. García-González, *Int. J. Mol. Sci.*, 2015, **16**, 17193–17230.
- 44 S. M. Choi, P. Chaudhry, S. M. Zo and S. S. Han, *Cutting-Edge Enabling Technologies for Regenerative Medicine*, 2018, pp. 161–210.
- 45 H. Su, Y. Zhang, Y. Liu, R. Lu, A. Gao, Q. Han, B. Wen, B. Hu and P. Yang, *Adv. Mater.*, 2023, **35**, 2300829.
- 46 T. P. Knowles, M. Vendruscolo and C. M. Dobson, *Nat. Rev. Mol. Cell Biol.*, 2014, **15**, 384–396.
- 47 M. R. Chapman, L. S. Robinson, J. S. Pinkner, R. Roth, J. Heuser, M. Hammar, S. Normark and S. J. Hultgren, *Science*, 2002, **295**, 851–855.
- 48 D. M. Fowler, A. V. Koulov, C. Alory-Jost, M. S. Marks, W. E. Balch and J. W. Kelly, *PLoS Biol.*, 2006, **4**, e6.
- 49 S. K. Maji, D. Schubert, C. Rivier, S. Lee, J. E. Rivier and R. Riek, *PLoS Biol.*, 2008, **6**, e17.
- 50 I. Cherny and E. Gazit, *Angew. Chem., Int. Ed.*, 2008, **47**, 4062–4069.
- 51 Y. Liu, S. Miao, H. Ren, L. Tian, J. Zhao and P. Yang, *Nat. Protoc.*, 2024, **19**, 539–564.
- 52 E. Eanes and G. Glenner, *J. Histochem. Cytochem.*, 1968, **16**, 673–677.
- 53 M. Sunde, L. C. Serpell, M. Bartlam, P. E. Fraser, M. B. Pepys and C. C. Blake, *J. Mol. Biol.*, 1997, **273**, 729–739.
- 54 A. S. Cohen and E. Calkins, *Nature*, 1959, **183**, 1202–1203.
- 55 R. Riek and D. S. Eisenberg, *Nature*, 2016, **539**, 227–235.
- 56 A. W. Fitzpatrick, S. T. Park and A. H. Zewail, *Proc. Natl. Acad. Sci. U. S. A.*, 2013, **110**, 10976–10981.
- 57 J. Hobbs and A. Morgan, *J. Path. Bact.*, 1963, **86**, 437–442.
- 58 H. Naiki, K. Higuchi, M. Hosokawa and T. Takeda, *Anal. Biochem.*, 1989, **177**, 244–249.
- 59 D. P. Steensma, *Arch. Pathol. Lab. Med.*, 2001, **125**, 250–252.
- 60 F. Chiti and C. M. Dobson, *Annu. Rev. Biochem.*, 2017, **86**, 27–68.
- 61 M. Baba, S. Nakajo, P.-H. Tu, T. Tomita, K. Nakaya, V. Lee, J. Q. Trojanowski and T. Iwatsubo, *Am. J. Pathol.*, 1998, **152**, 879.
- 62 D. M. Holtzman, J. C. Morris and A. M. Goate, *Sci. Transl. Med.*, 2011, **3**, 77sr71.
- 63 M. Jucker and L. C. Walker, *Ann. Neurol.*, 2011, **70**, 532–540.
- 64 K. Johnson, T. O'Brien, C. Betsholtz and P. Westermark, *Lab. Invest.*, 1992, **66**, 522–535.
- 65 D. M. Fowler, A. V. Koulov, W. E. Balch and J. W. Kelly, *Trends Biochem. Sci.*, 2007, **32**, 217–224.
- 66 S. K. Maji, M. H. Perrin, M. R. Sawaya, S. Jessberger, K. Vadodaria, R. A. Rissman, P. S. Singru, K. P. R. Nilsson, R. Simon and D. Schubert, *Science*, 2009, **325**, 328–332.
- 67 L. Li, C. P. Sanchez, B. D. Slaughter, Y. Zhao, M. R. Khan, J. R. Unruh, B. Rubinstein and K. Si, *Curr. Biol.*, 2016, **26**, 3143–3156.
- 68 L. Goldschmidt, P. K. Teng, R. Riek and D. Eisenberg, *Proc. Natl. Acad. Sci. U. S. A.*, 2010, **107**, 3487–3492.
- 69 J. W. Kinney, S. M. Bemiller, A. S. Murtishaw, A. M. Leisgang, A. M. Salazar and B. T. Lamb, *Alzheimers Dement (N Y)*, 2018, **4**, 575–590.
- 70 P. Hortschansky, V. Schroeckh, T. Christopeit, G. Zandomeneghi and M. Fändrich, *Protein Sci.*, 2005, **14**, 1753–1759.
- 71 M. P. Schützmann, F. Hasecke, S. Bachmann, M. Zielinski, S. Hänsch, G. F. Schröder, H. Zempel and W. Hoyer, *Nat. Commun.*, 2021, **12**, 4634.
- 72 A. Dehsorkhi, V. Castelletto, I. W. Hamley, J. Adamcik and R. Mezzenga, *Soft Matter*, 2013, **9**, 6033–6036.
- 73 Y. Song, T. Li, X. Zhang and L. Wang, *Food Biosci.*, 2023, **51**, 102068.
- 74 J. J. Kayser, P. Arnold, A. Steffen-Heins, K. Schwarz and J. K. Keppler, *J. Food Eng.*, 2020, **270**, 109764.
- 75 T. Li, J. Zhou, M. Peydayesh, Y. Yao, M. Bagnani, I. Kutzli, Z. Chen, L. Wang and R. Mezzenga, *Adv. Sustainable Syst.*, 2023, **7**, 2200414.
- 76 S. Mykolenko, W. L. Soon and R. Mezzenga, *Food Hydrocolloids*, 2024, **149**, 109604.
- 77 L. Hou, Y. Niu, Y. Wang, Y. Jiang, R. Chen, T. Ma and F. Gao, *NANO*, 2016, **11**, 1650063.
- 78 B. Hu, Y. Shen, J. Adamcik, P. Fischer, M. Schneider, M. J. Loessner and R. Mezzenga, *ACS Nano*, 2018, **12**, 3385–3396.
- 79 Y. Xu, Y. Liu, X. Hu, R. Qin, H. Su, J. Li and P. Yang, *Angew. Chem., Int. Ed.*, 2020, **59**, 2850–2859.
- 80 E. Andreetto, E. Malideli, L. M. Yan, M. Kracklauer, K. Farbiarz, M. Tatarek-Nossol, G. Rammes, E. Prade, T. Neumüller and A. Caporale, *Angew. Chem., Int. Ed.*, 2015, **54**, 13095–13100.
- 81 A. J. Doig and P. Derreumaux, *Curr. Opin. Struct. Biol.*, 2015, **30**, 50–56.
- 82 A. Romano, Y. Engelberg, M. Landau and U. Lesmes, *Food Hydrocolloids*, 2023, **136**, 108248.
- 83 P. Arghavani, S. Behjati Hosseini, F. Moosavi-Movahedi, S. Karami, M. Edrisi, M. Azadi, S. Azadarmaki and A. A. Moosavi-Movahedi, *ACS Appl. Mater. Interfaces*, 2024, **16**, 30997–31010.

- 84 G. Kabay, A. E. Meydan, G. K. Can, C. Demirci and M. Mutlu, *Mater. Sci. Eng., C*, 2017, **81**, 271–279.
- 85 T. Carvalho, R. Bártoło, A. Correia, C. Vilela, S. Wang, H. A. Santos and C. S. Freire, *Macromol. Rapid Commun.*, 2024, **45**, 2400129.
- 86 S. Das, R. Kumar, N. N. Jha and S. K. Maji, *Adv. Healthcare Mater.*, 2017, **6**, 1700368.
- 87 B. Hu, M. Li, X. He, H. Wang, J. Huang, Z. Liu and R. Mezzenga, *Biomater. Sci.*, 2022, **10**, 3597–3611.
- 88 J. Gu, Y. Su, P. Liu, P. Li and P. Yang, *ACS Appl. Mater. Interfaces*, 2017, **9**, 198–210.
- 89 J. Tian, Y. Liu, S. Miao, Q. Yang, X. Hu, Q. Han, L. Xue and P. Yang, *Biomater. Sci.*, 2020, **8**, 6903–6911.
- 90 Z. Wang, C. Fu, Y. Gao, Z. Wu, W. Chen, B. Hu, S. Xu, Z. Zhang and P. Yang, *Colloids Surf., B*, 2023, **225**, 113239.
- 91 Y. Liu, K. Li, J. Tian, A. Gao, L. Tian, H. Su, S. Miao, F. Tao, H. Ren and Q. Yang, *Nat. Commun.*, 2023, **14**, 5145.
- 92 J. Zhao, Y. Qu, H. Chen, R. Xu, Q. Yu and P. Yang, *J. Mater. Chem. B*, 2018, **6**, 4645–4655.
- 93 J. Du, Z. Guo, X. Yan, Y. Yao, R. Zhang, Y. Zhou, X. Liu, B. Shang, J. Huang and S. Gu, *Int. J. Biol. Macromol.*, 2025, **292**, 139124.
- 94 Y. Ha, J. Yang, F. Tao, Q. Wu, Y. Song, H. Wang, X. Zhang and P. Yang, *Adv. Funct. Mater.*, 2018, **28**, 1704476.
- 95 Y. Gao, Y. Pang, S. Wei, Q. Han, S. Miao, M. Li, J. Tian, C. Fu, Z. Wang and X. Zhang, *ACS Appl. Mater. Interfaces*, 2023, **15**, 10426–10440.
- 96 D. Wang, J. Deng, X. Deng, C. Fang, X. Zhang and P. Yang, *Adv. Mater.*, 2020, **32**, 2002080.
- 97 C. Li, D. Lu, J. Deng, X. Zhang and P. Yang, *Adv. Mater.*, 2019, **31**, 1903973.
- 98 D. Xu, J. Zhou, W. L. Soon, I. Kutzli, A. Molière, S. Diedrich, M. Radiom, S. Handschin, B. Li and L. Li, *Nat. Commun.*, 2023, **14**, 6806.
- 99 T. Li, J. Zhou, Q. Wu, X. Zhang, Z. Chen and L. Wang, *Food Chem.*, 2023, **398**, 133798.
- 100 X. Chen, J. Yi, Z. Wen and Y. Fan, *Food Hydrocolloids*, 2024, **149**, 109630.
- 101 Y. Fu, Y. Li, S. Weng, W. Qi, H. Su and T. Li, *Food Hydrocolloids*, 2023, **139**, 108581.
- 102 S. Mykolenko, M. Usuelli, A. Lustgarten, P. Fischer and R. Mezzenga, *Food Hydrocolloids*, 2025, 111491.
- 103 R. Zeng, Z. Liu, Z. Jiang, C. Xiao, Y. Zuo and J. Zhao, *Food Biosci.*, 2025, **64**, 105837.
- 104 L. Zheng, Z. Tian, B. Ai, Y. Yang, X. Zheng, Y. Liu, D. Xiao, Z. Sheng and J. Qin, *Food Hydrocolloids*, 2025, **163**, 111085.
- 105 Q. Yang, W. J. Ren, X. H. Yu, J. W. Zhang and H. Q. Chen, *Int. J. Biol. Macromol.*, 2025, **308**, 142704.
- 106 Y. R. Lai, T. L. Ho, Y. H. Yang, T. H. Lin and S. S. Wang, *Int. J. Biol. Macromol.*, 2025, 144817.
- 107 Y. Dong, T. Lan, L. Wang, X. Wang, Z. Xu, L. Jiang, Y. Zhang and X. Sui, *Food Chem. X*, 2023, **20**, 100995.
- 108 G. Liu, R. Liu, C. Fu, X. Hu, K. Li, L. Yan, P. Yang and J. Zhao, *Chem. Eng. J.*, 2025, 165048.
- 109 J. Li, J. Tian, Y. Gao, R. Qin, H. Pi, M. Li and P. Yang, *Chem. Eng. J.*, 2021, **410**, 128347.
- 110 H. Wang, Y. Huang, X. Liu, Z. Liu, K. Qian and L. Li, *Food Control*, 2025, 111498.
- 111 Q. H. Zhang, W. N. Yang, H. H. Ngo, W. S. Guo, P. K. Jin, M. Dzakupasu, S. J. Yang, Q. Wang, X. C. Wang and D. Ao, *Environ. Int.*, 2016, **92–93**, 11–22.
- 112 W. L. Soon, M. Peydayesh, R. Mezzenga and A. Miserez, *Chem. Eng. J.*, 2022, **445**, 136513.
- 113 D. D. Yang, F. X. Chang, B. F. Zhang and Y. C. Yong, *Bioresour. Bioprocess.*, 2024, **11**, 22.
- 114 W. Lu, C. Zhang, Z. Lin, X. Li, G. Zhao, Z. Qin, T. Zhang, Y. Li, W. Li and Y. Zhang, *Chem. Eng. J.*, 2023, **476**, 146561.
- 115 S. Zeng, Y. Wang, Y. Zhou, W. Li, W. Zhou, X. Zhou, M. Wang, X. Zhao and L. Ren, *Sep. Purif. Technol.*, 2022, **290**, 120856.
- 116 X. Jia, M. Peydayesh, Q. Huang and R. Mezzenga, *Small*, 2022, **18**, 2105502.
- 117 J. L. Tu, Y. R. Lai, C. Y. Lin, S. S. S. Wang and T. H. Lin, *Int. J. Biol. Macromol.*, 2024, **283**, 137680.
- 118 M. Peydayesh, J. Vogt, X. Chen, J. Zhou, F. Donat, M. Bagnani, C. R. Müller and R. Mezzenga, *Chem. Eng. J.*, 2022, **449**, 137703.
- 119 M. Peydayesh, E. Boschi, F. Donat and R. Mezzenga, *Adv. Mater.*, 2024, **36**, e2310642.
- 120 M. Peydayesh, T. Greber, I. Haechler, A. Armanious, X. Jia, M. Usuelli, M. Bagnani and R. Mezzenga, *Adv. Sustainable Syst.*, 2022, **6**, 2100309.
- 121 M. Bagnani, M. Peydayesh, T. Knapp, E. Appenzeller, D. Sutter, S. Kränzlin, Y. Gong, A. Wehrle, S. Greuter and M. Bucher, *Biomacromolecules*, 2024, **25**, 2033–2040.
- 122 N. Zhang, R. Shi, M. Zhou, P. Wang, Y. Yu and Q. Wang, *Int. J. Biol. Macromol.*, 2023, **247**, 125699.
- 123 F. Yang, Q. Yang, M. Chen, C. Luo, W. Chen and P. Yang, *Cell Rep. Phys. Sci.*, 2021, **2**, 100379.
- 124 Q. Yang, J. Zhao, A. Muhammad, R. Qin, J. Tian, L. Li, Q. Zhang, L. Chen and P. Yang, *J. Mater. Chem. A*, 2022, **10**, 14906–14916.
- 125 N. Feng, X. Guo, M. Chen, X. Chen, C. Li, L. Yan, P. Yang and J. Kong, *Sep. Purif. Technol.*, 2025, **367**, 132965.
- 126 Q. Yang, J. Zhao, Y. Zhang, X. Zhou, H. Ren, B. Hu, Z. Lei, L. Chen and P. Yang, *Sci. China Chem.*, 2024, **68**, 317–328.
- 127 Q. Yang, J. Cao, F. Yang, Y. Liu, M. Chen, R. Qin, L. Chen and P. Yang, *Chem. Eng. J.*, 2021, **416**.
- 128 F. Yang, M. Li, J. Xiong, X. Lv, X. Ma, W. Chen and P. Yang, *CCS Chem.*, 2025, **7**, 493–506.
- 129 C. Fu, Z. Wang, Y. Gao, J. Zhao, Y. Liu, X. Zhou, R. Qin, Y. Pang, B. Hu and Y. Zhang, *Nat. Sustainability*, 2023, **6**, 984–994.
- 130 S. Boyko, K. Surewicz and W. K. Surewicz, *Proc. Natl. Acad. Sci. U. S. A.*, 2020, **117**, 31882–31890.
- 131 S. Mukherjee, M. Poudyal, K. Dave, P. Kadu and S. K. Maji, *Chem. Soc. Rev.*, 2024, **53**, 4976–5013.
- 132 S. Ray, N. Singh, R. Kumar, K. Patel, S. Pandey, D. Datta, J. Mahato, R. Panigrahi, A. Navalkar and S. Mehra, *Nat. Chem.*, 2020, **12**, 705–716.
- 133 S. Wegmann, B. Eftekhazadeh, K. Tepper, K. M. Zoltowska, R. E. Bennett, S. Dujardin, P. R. Laskowski, D. MacKenzie, T. Kamath and C. Commins, *EMBO J.*, 2018, **37**, e98049.
- 134 Y. Xing, A. Nandakumar, A. Kakinen, Y. Sun, T. P. Davis, P. C. Ke and F. Ding, *J. Phys. Chem. Lett.*, 2020, **12**, 368–378.
- 135 S. Sudhakar, A. Manohar and E. Mani, *ACS Chem. Neurosci.*, 2023, **14**, 3655–3664.